Mapping of a buried basement combining aeromagnetic, gravity and petrophysical data: The substratum of southwest Paris Basin, France

Julien Baptiste, Guillaume Martelet, Michel Faure, Laurent Beccaletto, Pierre-Alexandre Reninger, José Perrin, Yan Chen

Mapping of a buried basement combining aeromagnetic, gravity and petrophysical data: the substratum of southwest Paris Basin, France

*Julien Baptiste[1,2], Guillaume Martelet[2], Michel Faure[1], Laurent Beccaletto[2], Pierre-Alexandre Reninger[2], José Perrin[2], Yan Chen[1],

[1] Institut des Sciences de la Terre d'Orléans, UMR 7327, Université d'Orléans, Campus Géosciences, 1A rue de la Férollerie, 45071 Orléans Cedex 2

[2] Bureau de Recherche Géologique et Minière (BRGM), UMR 7327, 3 avenue Claude Guillemin, BP 36009, 45060 Orléans Cedex 2.

* Corresponding author: j.baptiste@brgm.fr

Abstract

Aeromagnetic and gravity data have proven to be among the most effective methods for mapping deeply buried basin/basement interfaces. However, the data interpretation generally suffers from ambiguities, due to the non-uniqueness of the gravity and magnetic signatures. Here, we tie the gravity and magnetic signatures with a petrophysical characterization of the lithologies outcropping around the French Paris Basin. Our methodology investigates the lithology and structure of its hidden Variscan substratum at the junction between the Armorican Massif and Massif Central. Our approach is based on the combination of potential field data, magnetic susceptibilities measured in the field, density values of sample rocks and information documented in boreholes, in order to propose a new interpretative geological map of the buried substratum of the Paris Basin. The petrophysical description is combined with geophysical patterns of the substratum, mapped through statistical unsupervised classification of suitably selected magnetic and gravity maps. The first step of interpretation consists in extending the outcropping major structures below the Meso-Cenozoic sedimentary cover of the Paris Basin. The litho-structural units, in between these major structures, are then interpreted separately. The second step consists in assigning lithologies within each unit, with respect to its magnetization and density (as derived from the petrophysical compilation), and mapping its extension under cover, integrating punctual borehole information. Overall, with a special emphasis on relating geophysical signatures and petrophysical characteristics of litho-structural units, this methodology permits a precise structural and lithological cartography of a segment of the buried Variscan substratum. In the southwestern part of the Paris Basin, this approach reveals: i) the limited eastward extension of Central Brittany, ii) the eastward extension of the major Cholet fault, iii) the emphasis on N150E-N160E striking fault and

their N30E conjugates, controlling the opening of Permo-Carboniferous basins, and iv) the eastward extension of the Eo-Variscan suture.

Keywords: aeromagnetic, gravity, Paris Basin, Variscan substratum, petrophysical data, undercover mapping

1. Introduction

The European Variscan belt belongs to a several thousand-km-long Late Paleozoic orogen extending from the Appalachians in the eastern North America, to Polish Sudetes, through the Mauritanides in West Africa. This belt, formed by Proterozoic to Carboniferous rocks, constitutes the Pre-Mesozoic basement of a large part of Western and Central Europe. In France, the Variscan belt presently crops out in several massifs, namely: Massif Central, Armorican, Ardennes, and Vosges Massifs and in the basement of the Cenozoic Alpine and Pyrenean belts. The continuity between these massifs is hidden by several Mesozoic to Cenozoic sedimentary basins, such as the Paris or Aquitaine Basin (Fig. 1)

The Paris Basin is an intraplate sedimentary basin, set up on the Variscan substratum that crops out in the above massifs (Pomerol, 1978; Mégnien; 1980, Perrodon and Zabek, 1990; Guillocheau et *al.*, 2000; Chantraine et *al.*, 2003) (Fig. 1). It is well known that lithologies and structures of the southern part of the Armorican Massif and the Massif Central are closely related (Autran and Lameyre, 1980; Matte and Hirn, 1988; Virlogeux et *al.*, 1999; Faure et *al.*, 2005; Cartannaz et *al.*, 2006; Gébelin et *al.*, 2007; Ballèvre et *al.*, 2009; Rolin et *al.*, 2009); however, their connection is still poorly known, as it hidden by the Meso-Cenozoic Paris Basin sedimentary cover. Both massifs are composed of several litho-tectonic units separated by crustal-scale shear zones, such as the North Armorican Shear Zone (NASZ) and the South Armorican Shear Zone (SASZ), in the Armorican Massif or the Marche Fault in the Massif Central (Fig. 1). In addition, the Nort-sur-Erdre fault of the

Armorican Massif (NSE F.; Fig. 1) is acknowledged as the Eo-Variscan suture (Fig. 1) (Matte, 1986; Le Corre et *al.*, 1991; Ballèvre et *al.*, 1992; Lardeux and Cavet, 1994; Faure et *al.*, 1997; Cartier et *al.*, 2001; Bitri et *al.*, 2003). The eastward extension of the Armorican litho-structural units has already been integrated in large-scale geodynamic reconstructions of the Variscan belt, either based on geological evidence (e.g. Matte, 1986; Faure et *al.*, 2005; Ballèvre et *al.*, 2009; Martínez-Catalán, 2012, Edel *et al.*, 2015) or on low to medium-resolution regional geophysics (e.g. Edel, 2008). There is no agreement on the limits and nature of the units, and geodynamic significance is still under debate. A way to ascertain these models would be to fill the geological observation gap caused by the Meso-Cenozoic sedimentary cover of the Paris Basin by new high resolution data.

In the second half of the 20th century, the Paris Basin substratum started being investigated using gravity data (Goguel and Francia, 1954), deep boreholes (Lienhardt, 1961) or deep seismic profiles (Matte and Hirn, 1988). A combination of gravity and intermediate to low resolution aeromagnetic data was used in the southwestern part of the Paris Basin (Weber, 1973). The extension of this last study to the entire Paris Basin led to the first version of a pseudo-lithological and structural sketch of the pre-Mesozoic substratum of the Paris Basin (Debeglia and Weber, 1980). More recently, on the basis of the combination of new high resolution magnetic data and updated gravity data, Martelet et *al.*, (2013) proposed a method to characterize the substratum geometry of the central-south part of the Paris Basin, but no detailed lithological interpreted map was produced yet.

In addition, a map of the buried substratum around the Poitou High was proposed on the base of detailed structural analysis and drilling information (Rolin and Colchen, 2001). Because we now benefit from recent high resolution aeromagnetic data on the entire southwestern part of the Paris Basin, we are now able to address the litho-structural pattern of its buried substratum with an unprecedented resolution. Complemented by a characterization of the field petrophysical properties of the various litho-structural units, our work ascertain cartographic interpretations of the geophysical signatures. Our methodology emphasizes the processing of interpretation of potential field data to derive a high-resolution structural map. Combining the latter with field petrophysical properties, lithologies were then interpreted in each litho-structural unit, leading to a new geological map of the Paris Basin substratum.

The extensions of the litho-structural units as well as the lithologies of the Variscan and their regional geological implications are further discussed.

2. Geological setting

The Paris Basin is a low subsidence Meso-Cenozoic sedimentary basin. It is composed of silico-clastic and calcareous rocks (Pomerol, 1978; Mégnien, 1980; Perrodon and Zabek, 1990; Guillocheau et *al.*, 2000; Beccaletto et *al.*, 2011)***.*** It is set up on a Variscan substratum including Permo-Carboniferous basins. In the study area, the formations constituting the Variscan substratum of the Paris Basin laterally outcrop in the Armorican Massif to the west and the Massif Central, to the south, respectively (Fig. 2a).

The Armorican Massif is composed of several litho-structural units separated by crustal-scale faults and characterized by distinct lithologies and tectonic evolutions (Fig. 2a). The North Armorican Shear Zone (NASZ; Chauris, 1969; Watts and Williams, 1979), the northern and the southern branches of the South Armorican Shear Zone (NBSASZ and SBSASZ, respectively) (Jégouzo, 1980) and the Nort-sur-Erdre fault (NSE) are the main Variscan structures of the central and southeastern part of the Armorican Massif (Fig. 2a). The NASZ and the SBSASZ delimit the Central Brittany to the north and south, respectively (Fig. 2a). Central Brittany consists of folded and weakly metamorphosed Neoproterozoic sediments, unconformably overlain by weakly deformed Paleozoic sediments, intruded by Carboniferous granites (Fig. 2b) (Vernhet et *al.*, 2009). Located along the NASZ, the southerly early Carboniferous Laval basin is superimposed on the Neoproterozoic to Paleozoic series (Fig. 2b). It is composed of early Carboniferous sedimentary rocks interbedded with acidic and basic volcanic rocks (Le Hérissé and Plaine, 1982). The Laval basin was folded during the Late Carboniferous (Houlgatte *et al.*, 1988).

Between the NBSASZ and the NSE fault, the Paleozoic series of the St-Georges-sur-Loire unit overthrusts to the NW the Lanvaux unit (Fig. 2a). The NW-SE striking Lanvaux unit is composed of Neoproterozoic and early Cambrian metasediments overlain by Paleozoic weakly metamorphosed sediments (Lardeux and Cavet, 1994), and intruded by an early Ordovician granite deformed into an orthogneiss (Fig. 2b), called the St-Clément-de-la-Place (Vidal, 1980). This orthogneiss is intruded by two granitic plutons: i) the Bécon granite (Chauris and Lucas, 1964; Cavet et *al*., 1970, 1976) and ii) the St-Lambert granodiorite showing S/C structures, emplaced during to the Carboniferous dextral shearing of the NBSASZ (Faure and Cartier, 1998). The Lanvaux unit experienced a polyphase deformation (Faure and Cartier, 1998). The foliation attitude documents an antiform, the core of which is constituted by the orthogneiss. Outcropping at the junction between the Lanvaux and St-Georges-sur Loire unit, the Questembert leucogranite, emplaced during the late Carboniferous (Tartèse et *al*., 2011a, 2011b) is a syn-tectonic granite related to the SASZ shearing (Berthé et *al*., 1979; Bernard-Griffiths et *al.*, 1985).

To the south, the St-George-sur-Loire unit is divided into two sub-units (Fig. 2a): the blocky sub-unit in the south overthrusts to the NW the northerly Sandstone-Pelite sub-unit (Cartier et *al.*, 2001; Cartier and Faure, 2004).

The south of Nort-sur-Erdre fault is a metamorphic nappe stack: described in the southern part of the Armorican Massif (Burg, 1981; Matte, 1991; Bosse et *al.*, 2000; Le Hébel et *al.*,

2002) and in the northern part of the Massif Central (Quenardel and Rolin, 1984; Faure et *al.*, 1990). The structure and the lithology of the metamorphic Champtoceaux Complex in the Armorican Massif and of the Aigurande Plateau in the Massif Central are quite similar (Fig. 2b) (e.g. Faure et *al.*, 2005; Ballèvre et *al.*, 2009). However the Armorican Massif exposes peculiar units absent in the Massif Centr*al.* The uppermost unit of the nappe stack, called the Mauges nappe (Fig. 2a), consists of Neoproterozoic metagrauwackes interbedded with meta-volcanics (Wyns and Le Métour, 1983; Cabanis and Wyns, 1986; Wyns et *al.*, 1998), and unconformably overlain by Cambrian sedimentary rocks and felsic volcanites, and Ordovician sandstones (Fig. 2b). This Paleozoic sedimentary and volcanic series is widely exposed in the Choletais area (Cavet et *al.*, 1966). The Cambrian Thouars micrograniitic massif associated with basic rocks (gabbros, quartz diorites) intrudes within the Neoproterozoic micaschists, the volcanic series and the dyke complex (Fig. 2b; Thiéblemont et *al.*, 1987, 2001). To the north of the Mauges nappe, the Ancenis basin is located along the NSE fault (Fig. 2a). It is made of Devonian to early Carboniferous deposits (Fig. 2b) (Cavet et *al.*, 1971; Ballèvre and Lardeux., 2005), superimposing the Neoproterozoic micaschists (Fig. 2b).

Another unit, exposed uniquely in the Armorican Massif is the "Drain Unit" consisting of serpentinite, gabbro, basalt and siliceous sedimentary rocks, interpreted as dismembered ophiolites along the Eo-variscan suture (Marchand, 1981; Ballèvre et *al.*, 1994; Faure et *al.*, 2008). The underlying unit, called the Champtoceaux complex, is an imbrication of crustal-scale thrust sheets characterized by highly deformed and metamorphosed gneiss and eclogites (Marchand, 1981; Ballèvre et *al.*, 1989, 1994; Bosse et *al.*, 2000). Lastly, the lowermost unit exposed in this area consists of a micaschist and paragneiss suite, named the Mauves-sur-Loire series (Fig. 2b). The entire stack of nappes from the Mauges nappe to the Mauves-sur-Loire series is folded in a km-scale antiform with a steeply eastward plunging axis probably related to the dextral shearing of the SASZ (Martelet et *al.*, 2004). Carboniferous plutons occupy the core of this antiform (e.g. Wyns et *al.*, 1998).

The Aigurande Plateau also consists of a stack of metamorphic nappes, refolded as an ENE-SSW striking antiform, and intruded by several two-mica granitic plutons (Quenardel and Rolin, 1984; Faure et *al.*, 1990). From top to bottom, the litho-tectonic units are characterized by: i) the Upper Gneiss Unit (UGU) composed of a bimodal magmatic series, named leptynite-amphibolite complex with eclogites, and migmatites; ii) the Lower Gneiss Unit (LGU) made of metagrauwackes, micaschists, metarhyolites and amphibolites that never experienced a HP metamorphism; iii) the Para-autochthonous Unit composed of low-grade micaschists (Fig. 2b). The left-lateral Marche fault, main Variscan structure of the northern part of the Massif Central (e.g. Quenardel and Rolin, 1984), is the southern boundary of the Aigurande Plateau (Fig. 2a). A reasonable correlation between the Champtoceaux Complex and the Mauves-sur-Loire Unit in the Armorican Massif and the UGU and LGU in the Massif Central, respectively has been proposed (e.g. Faure et *al.*, 2005).

Previous structural and lithological analyses within the Poitou High (Rolin and Colchen, 2001) documented the close connection between the Haut Bocage unit and the Confolentais area. In the Poitou High, the substratum that crops out in rare valleys is made of Carboniferous granite. Below the sedimentary cover of the Poitou High, the SBSASZ eastward extension splits into several branches which separate structures and lithologies of the Haut Bocage and Confolentais units (Fig. 2a) (Rolin and Colchen, 2001). The Haut Bocage unit is composed of anatectic gneiss and Neoproterozoic micaschists (Fig. 2b). The Confolentais unit is made of granites, metavolcanites and metasediments belonging to the UGU (Fig. 2b). Both units are intruded by late Devonian gabbro, granodiorites and diorites that also crop out along the left-lateral Marche fault (Peiffer, 1986; Cuney et *al.*, 1993; Pin and Paquette, 2002). In the Confolentais area can be found the westernmost expression of the Limousin tonalite belt (Bernard-Griffiths et *al.*, 1985; Peiffer, 1986).

3. Aeromagnetic and gravity data

3.1. Processing of aeromagnetic data

Magnetic measurements monitor the spatial variations of magnetic properties of the underground, from the surface of the Earth down to several kilometers. The French Geological Survey (BRGM) conducted a fixed-wing magnetic survey in 1998 over Brittany (Bonijoly et *al.*, 1999; Truffert et *al.*, 2001) and from August 2008 to October 2010 over the Pays de la Loire (PaL) and Région Centre (Martelet et *al.*, 2013) covering the Armorican Massif and the southwestern part of the Paris Basin (Fig. 3a). These surveys were flown at an average 85 m and 120 m ground clearance for Région Centre, PaL and Brittany, respectively. For the three surveys, the flight path was oriented N-S, with a line-spacing of 500 m reduced to 250 m over key areas for the Brittany survey and 1 km reduced to 500 m for PaL and Région Centre surveys; perpendicular control tie lines were also flown every 10 km. The surveys overlap with each other on a 3 to 5 km band at their periphery. In order to get rid of punctual artifacts related to human activities, the data were upward continued to an elevation of 600 m. This removed the short wavelength cultural noise without significantly smoothing the data, with regards to the aims and regional extent of the study. Magnetic anomaly 250 m regular grids were produced using the minimum curvature gridding method (Taylor and Mason, 1972), separately, for each survey.

In addition three grid transforms were applied to emphasize various properties of the buried substratum:

- The reduction to the pole (RTP; Fig. 3b): it contributes to simplify the magnetic signal interpretation (Blakely, 1996). Taking into account the Earth field direction, this operator relocates the magnetic anomaly on top of its causative body. When induced magnetization predominates, anomaly bipolarities are removed, so that RTP positive anomalies indicate a local increase of magnetic susceptibility at depth.

- The vertical derivative (Fig. 3c): it enhances local signal gradients while regional trends are removed. Magnetization in the Meso-Cenozoic Paris Basin is weak and sedimentary cover thickness vary smoothly over large distances; therefore, they generate long wavelength components in the magnetic map, which are removed by the vertical gradient operator. Consequently the map of the magnetic vertical gradient highlights the magnetic contrasts within the underlying substratum (e.g. Weber, 1973; .Martelet et *al.*, 2013).
- The Tilt derivative (TILT) or Tilt angle processing (e.g. Miller and Singh, 1994; Verduzco et *al.*, 2004) is powerful for structural interpretation as it depicts equally the edge of deep and shallow magnetic sources (Miller and Singh, 1994). It is an effective method for mapping contacts or faults, weakly contrasted magnetized bodies, located under a sedimentary cover (Fairhead et *al.*, 2011). The TILT map was used to highlight the structures of the underlying substratum and the magnetic body contours which are defined by the zero value in the TILT map (Fig. 3d).

The vertical derivative and the tilt derivative operators were applied on the anomaly reduced to the pole (RTP). In order to avoid artifacts at survey junctions, the magnetic transforms were applied separately, survey by survey, before merging. The merge of the three magnetic surveys was carefully achieved, using a standard grid stitching algorithm.

3.2. Processing of gravity data

Gravity data derive from the compilation of ground gravity surveys conducted in France since the middle of the 20th century and compiled in the Banque Gravimétrique de la France (BGF) (Martelet, et *al.*, 2009). In the study area, the average station coverage is about 1 station/km². Data are tied to the CGF65 base station network. In order to derive the Bouguer anomaly, all standard corrections are included, with a reference density of 2600 kg/m3, and terrain corrections computed to a distance of 167 km (Martelet et *al.*, 2002). Taking into account the accuracy of 1) the network, 2) the gravity measurements and their positioning and 3) the terrain corrections, the RMS error on the Bouguer anomaly is 0.32 mGal in the study area. The Bouguer anomaly map presented in Fig. 4a locates the main regional density contrasts, from the surface down to several kilometers at depth.

A map of the vertical derivative of the Bouguer anomaly is presented in Fig. 4b. The first order of the vertical gradient of the Bouguer anomaly has long been used for separating close structures (Elkins, 1951; Gérard and Griveau, 1972; Goguel, 1972). Here, this operator is used to highlight density contrasts within the Paris Basin substratum. As for the magnetic map, the regional effect of the Meso-Cenozoic sedimentary pile results in smooth and long wavelength signals and is therefore strongly attenuated by this operator (see Martelet et *al.*, 2013 for more details). Positive and negative signals of the vertical gradient feature relatively high and low density rocks at depth, respectively.

4. Measurements of field rock properties

Gravity and magnetic map usually display “averaged” geophysical signatures of geological bodies as compared to the lithological variations at the outcrop scale; the discrimination of the magnetic and gravity causative lithologies suffering from ambiguities. An extensive campaign of petrophysical sampling and measurements was conducted in order to take into account this scale effect in our geophysical maps interpretation. It was designed to derive reliable petrophysical "statistic signatures" for the main lithologies encountered in the study area.

4.1 Magnetic susceptibility

The magnetic susceptibility of a rock refers to its ability to become magnetized by an external magnetic field such as the Earth's field (e.g. Dearing, 1999). Rocks have various magnetic responses due to their magnetic properties, which to the first order, depend on the volume content of magnetite (Clark and Emerson, 1991). Magnetic susceptibility field measurements were carried out using a hand-held kappameter (KT-9, Exploranium, Canada). The measuring range of KT-9 susceptibility meters is from -999 to 999 x 10–3 SI units with a sensitivity of 1 x 10-5 SI. Because reproducibility of measures is influenced by the irregularity of the rock surface (Lecoanet et *al.*, 1999), measures were achieved in the "Pin-mode" of the kappameter which takes into account a geometric factor to reduce roughness effects.

About 4050 magnetic susceptibility measurements were taken directly on 130 outcrops, all along the southeastern border of the Armorican Massif and the northwestern border of the Massif Central and Poitou High (Fig. 3a). Within each litho-structural unit, most of the outcropping lithologies were sampled. The compilation of these measurements is presented in Fig. 5. For each litho-structural unit, we numerated the magnetic susceptibility measurements within constant intervals of variation. In Fig. 5, the colored bars highlight the most represented magnetic susceptibility ranges, whereas the grey intervals indicate ranges with few randomly distributed data.

As an aid for the interpretation, the magnetic susceptibility was subdivided into three representative ranges, based on the classification of Clark and Emerson (1991) and the separation range of Théveniaut and Clarke, (2013): i) from negative values to 4 x 10-4 SI, ii) from 4 x 10-4 to 5 x 10-3 SI and iii) above 5 x 10-3 SI, designated as low, intermediate and high magnetic susceptibility ranges, respectively. Fe-rich sandstones in Central Brittany exhibit the highest magnetic susceptibility of the study area (Fig. 5). Basic rocks (gabbro-diorite, granodiorite and amphibolite), and Cambrian felsic volcanites are also within the high magnetic susceptibility range, due to their high amount of ferrimagnetic minerals, such as magnetite, in their mineralogical composition (Thiéblemont et *al.*, 2011). Granite, leptynite, orthogneiss, migmatite, Neoproterozoic metasedimentary and Paleozoic sedimentary rocks, micaschists and metasediments are within the low magnetic susceptibility range, given that they are mainly composed of diamagnetic (quartz, plagioclase) and paramagnetic minerals. Some Paleozoic sedimentary rocks, basalts, metabasites, meta-gabbro, diorites and amphibolites are within the intermediate range, since they contain paramagnetic minerals, and a small amount of iron-bearing minerals (amphibole, biotite or clay minerals).

Induced magnetization is predominant in the area, but several bimodal anomalies in the RTP map (Fig. 3b) indicate some remnantly magnetized rocks. To the north, the Fe-rich Ordovician sandstones of Central Brittany, mainly composed of magnetite, have been studied in detail (Corpel and Weber, 1970): their Koenigsberger ratio is around 6 but the remnant component of magnetization is almost collinear to the ambient magnetic field and therefore does not strongly affect the mapping of this unit. Also, the granodiorite within the Choletais area and the diorite plutons within the Confolentais area are partly remnantly magnetized, but their magnetic anomalies almost perfectly match their field cartographic limits (Fig. 3b). This suggests that i) the effect of the remnant magnetization is weak, or ii) their direction of remnant magnetization is close to the induced magnetization. In these three cases, the location of the magnetic causative bodies is only slightly affected by the remnant magnetization and these lithologies also display a high magnetic susceptibility in the field (Fig. 5). Consequently, we made the assumption that the interpretation of the magnetic maps could be achieved considering the magnetic susceptibility only.

Globally, there is a significant overlap between the magnetic susceptibility ranges of the various lithologies; however, this overlap is rather limited between lithologies within each litho-structural unit. This observation is crucial for the geophysical maps interpretation, as described in the following paragraphs.

4.2 Density

Density is the petrophysical property influencing the gravity data. For this study, 54 unweathered rock samples from most of the lithologies were collected all along the Armorican and Massif Central borders in 48 outcrops (Fig. 3a). The densities of these samples were measured using the double weighting method, with a ca. 0.01 g/cm^3 uncertainty. The density determination of some lithologies was not possible due to bad outcropping conditions. In this case, a density value was affected with respect to the density average of the same lithology in the other litho-structural units.

As for the magnetic susceptibilities, the densities were subdivided into three representative groups: i) from 2.55 to 2.65 g/cm^3, ii) from 2.65 to 2.8 g/cm^3, and iii) above 2.8 g/cm^3 for low, intermediate and high densities, respectively (e.g. Edel, 2008) (Fig. 5).

5. Geophysical signatures of the Paris Basin substratum

The previous studies investigating the substratum of the Paris Basin using magnetic and gravity data manually outlined the main geophysical anomalies. They were interpreted with simplified lithological attributions, based on the substratum nature documented in some boreholes as well as some rock property data (Weber, 1973; Debeglia and Weber, 1980). More recently, Martelet et *al.*, (2013) proposed a map of petrophysical signatures of the substratum of the south-central part of the Paris Basin, based on a numerical classification combining gravity and magnetic data. We used the same approach to achieve a simplified magnetic-gravity signature of the substratum of the study area.

We agree with previous studies that considered the magnetic effect of the Meso-Cenozoic sedimentary cover of the Paris Basin, almost "transparent" for the magnetic field (Weber, 1973); therefore the magnetic map mostly features the buried substratum. Nevertheless the Meso-Cenozoic sedimentary pile at least attenuates the intensity of the magnetic response of the substratum and increases the wavelength of the substratum anomalies, as the sedimentary cover gets thicker; from 0 to about 2000m in the study area. The gravity field contains both the effects of the substratum and of the sedimentary basin. The vertical gradient of the Bouguer anomaly used for our classification attenuates the long wavelengths of the Meso-Cenozoic sedimentary pile (Debeglia and Weber 1985; Martelet et *al.*, 2013). Aiming at the same goals as Martelet et *al.*, (2013), the map of the magnetic anomaly reduced to the pole that was introduced in our classification, followed two considerations: 1) displaying information of the structure and magnetization of the substratum as detailed as possible; 2) being physically as homogeneous as possible with the gravity first vertical derivative. We added a third consideration: 3) reducing as much as possible the variable smoothing and attenuating effect of the Meso-Cenozoic sedimentary pile. Combining the characteristics of RTP and the TILT fulfils the three conditions. These two magnetic maps were combined with the vertical gradient of the Bouguer anomaly to obtain synthetized signatures of magnetic and gravity data. The three layers were combined into a ternary image, using a standard image fusion procedure. We then performed a numerical classification of this ternary image using unsupervised isodata clustering (e.g. Venkateswarlu and Raju, 1992). Based on their gravity and magnetic signatures, all pixels of the map were statistically distributed among 6 classes (Fig. 6a) which well figure the geophysical signatures of the outcropping geology. This map displays self-consistent cartographic bodies, which are compatible with known geological patterns. It features 2 levels of magnetic intensity (from light to dark green) and an intermediate average magnetic/gravity signature (in white) as well as 3 levels of gravity intensity (from light to dark blue). These synthetized geophysical signatures can be related to the simplified 3-levels categorization of the petrophysical magnetization/density parameters (Fig. 5). This map combines magnetic and gravity signatures and it is used as a support for the following structural and lithological interpretations.

6. Geological map of the pre-Mesozoic substratum

The first step of the interpretation consists in extending below the Paris Basin sedimentary cover the major structures recognized in the field (Fig. 2a) in order to delineate the Variscan litho-structural units under cover. The structural interpretation (Fig. 6b) uses all geophysical enhanced maps presented in Section 3 supported by the synthetized geophysical signatures map (Fig. 6a). The second step consists in interpreting the lithological nature of the hidden substratum, using the combined petrophysical characteristics of rocks (Fig. 5), the synthetized geophysical signatures of the substratum (Fig. 6a) and the structural sketch map including available boreholes (Fig. 6b).

6.1 Undercover delineation of structural features

Manually interpreted geophysical trends deriving from the magnetic and gravity maps are outlined in red in Fig. 6a. They underline the N110E-N120E and N90E striking structural directions of the Armorican Massif and the Massif Central, respectively, known in the field. In addition to these trends, main geophysical structures and discontinuities were interpreted. The interpretative structural map (Fig. 6b) showing the extension of the structural units below the Paris Basin cover is discussed from north to south.

Central Brittany is limited to the north by the NASZ. Its extension constitutes the northern limit of the study area; it is defined regionally by a major N110°E-oriented disharmony between the strong magnetic signals of Central Brittany to the south, and the northern weak magnetic signals (Fig. 3b). It also outlined by a successive E-W striking chaplet of magnetic anomalies bounded the NASZ to the north, which can be outlined from the field to the easternmost part of the studied area (Baptiste et *al.*, 2015) (Fig. 3c, Fig. 3d). The Lanvaux unit is marked by a well-defined NW-SE striking elongated low density anomaly, known as Lanvaux orthogneiss (Fig. 4b); it is bounded to the north by the NBSASZ. Following the magnetic and gravity trends under cover (Fig. 6a), the strike of the NBSASZ changes eastwards from NW-SE to NE-SW and joins the NASZ, limiting Central Brittany to the east (Fig. 6b). The southern border of the noticeable Lanvaux low gravity anomaly defines the limit between the Lanvaux unit and the northern part of St-Georges-sur-Loire unit (Fig. 6b).

In the field, the St-Georges-sur-Loire unit is characterized by low magnetic (Fig. 3b) and gravity signal (Fig. 4b), and by scattered moderate intensity magnetic anomalies (Fig. 3c) and a high intensity gravity anomaly, to the north and south, respectively. Predominant NW-SE/E-W striking geophysical trends are also observed (Fig. 6b). Under the Paris Basin sedimentary cover, the northern and southern part cannot be separated by geophysical data. The southern border of the high intensity gravity anomaly defines the southern limit of the St-Georges-sur-Loire unit (Fig. 4b); it defines the cartographic trace of the NSE Eo-Variscan suture (Fig. 6b).

The Choletais area, marked by an E-W striking high gravity elongated anomaly, extending 150km eastwards below the Paris Basin sedimentary cover (Fig. 4b), is bounded to the south, by the northern branch of the Cholet fault (Fig. 6b). This noticeable anomaly defines the southward boundary of the Mauges nappe. Along this fault, the magnetic and gravity trends strike E-W in continuity along more than 150 km (Fig. 6a). Northwards, the geophysical trends become less and less continuous (Fig. 6a), suggesting the decreasing gradient of deformation away from the fault, as observed in the Armorican Massif (Thiéblemont et *al.*, 2011). To the east (around 2°E), the E-W striking Cholet fault marks the northern limit of NW-SE geophysical trends of the Aigurande Plateau. Altogether, these features suggest that the Cholet fault can be considered as a major shear zone.

In the east of the study area (around 2°E), the NSE fault and the northern branch of the Cholet fault almost meet, closing the Mauges nappe and the Choletais area, to the east (Fig. 6a). To the south of the Cholet fault, low gravity anomalies (Fig. 4b) and signatures (Fig. 6a) and NW-SE striking geophysical trends (Fig. 6a) are predominant; this refers to the Haut Bocage unit and Confolentais area connection. To the east of the Haut Bocage unit, the direction of geophysical trends progressively changes from NW-SE to E-W, featuring the connection between the Haut Bocage unit and Aigurande Plateau.

In the easternmost part of the studied area, all these units are interrupted by NE-SW striking structures bounding the Permo-Carboniferous Contres basin, well characterized on seismic profiles and in deep boreholes (Fig. 6b; Beccaletto et *al.*, 2015).

At the regional scale, all structures are offset by N150E-N160E-striking faults and, to a lesser extent, by their conjugate N20E-N30E striking faults (Fig. 6b). In agreement with Martelet et *al.*, (2013), two kinematics are interpreted along the N150E-N160E faults: i) a dextral motion highlighted by the offset of preexisting structures and lithological markers, and ii) a vertical movement documented by the attenuation and the spreading of the magnetic signal from west to east. In the southeastern part of the Armorican Massif, the N150E striking Partenay fault is described as a middle to upper Visean dextral shear zone (Rolin et *al.*, 2009). The seismic information confirms the role of these faults during the opening of Carboniferous or Permian Arpheuilles and Contres basins (Fig. 6b; Beccaletto et *al.*, 2015). Moreover, they were interpreted as Permian or Triassic fracture zones reactivated during the opening of the North Atlantic Ocean and Gulf of Biscaye (Vigneresse, 1988). They are also known throughout the Armorican Massif, where they bound small Tertiary basins. Based on these information, the N150E-N160E striking faults can be interpreted as Variscan faults, reactivated during the tectonic evolution of the Paris Basin, strongly affecting present-day geometry in the southwestern part of the basin.

The N30E striking normal faults, mainly located in the Mauges nappe (Fig. 6b), are also interpreted as Variscan structures reactivated during the Permo-Carboniferous, controlling the geometry of the Arpheuilles basin (Fig. 6b; Beccaletto et *al.*, 2015).

6.2 Interpretation of the undercover lithologies

Based on the geophysical signatures and the structural information, we propose a geological map displaying the interpreted lithologies assigned to the dominant geophysical signatures (Fig.7a) and an interpretative cross section based on geological information observed in the field (Fig. 7b). This geological map as well as its tectonic implications are discussed in each litho-structural unit.

6.2.1 Central Brittany

Central Brittany is mainly composed of Neoproterozoic metasedimentary rocks and Paleozoic sedimentary rocks intruded by Carboniferous granites (Fig. 2). In this litho-structural unit, high magnetization and density signatures (Fig. 6a) unambiguously refer to the Fe-rich Ordovician sandstone (up to 0.8 SI and 3.11 g/cm^3; Fig. 5). This marker extends eastwards, bounding the NBSASZ (Fig. 8a); its presence is confirmed at 300m depth under cover by a borehole (Fig. 6b).

Contrary to previous models (Weber, 1971, 1973; Debeglia and Weber, 1980), the Paleozoic rocks can be discriminated from the Neoproterozoic ones using the petrophysical information. Paleozoic rocks including Fe-rich sandstones displaying low magnetization and density (from 1.5 to 5 x 10^{-4} SI and 2.71 g/cm^3; Fig. 5) can be traced eastwards (Fig. 7a). In the field, geophysical signatures of the Neoproterozoic metasedimentary rocks are heterogeneous, with intermediate magnetic susceptibility and low density (from 10^{-4} to 3 x 10^{-4} SI and 2.55 g/cm^3; Fig. 5). They are also intruded by moderately magnetic and dense (3.11 g/cm^3) gabbroic dykes (Verhnet et *al.*, 2009). Thus the map exhibits a succession of thin E-W trends with intermediate to high magnetic and intermediate gravity signatures that can be identified under the sedimentary cover and grouped with the Neoproterozoic metasedimentary rocks (Fig. 6a). The Laval basin has intermediate to low magnetic and gravity signatures as well as peculiar E-W trending texture (Fig. 6a) well visible in the magnetic vertical gradient (Fig. 3c). This E-W trending signature is likely related to interbedded basalts with intermediate magnetization and density (up to 10^{-2} SI and 2.85 g/cm^3; Fig. 5) as observed in the field (Fig. 8b). This feature allows delimiting the southern extension of the Laval basin under the Paris Basin cover (Fig. 8b). Furthermore, the low magnetic and gravity signatures (Fig. 6a) are related to Carboniferous granite intrusions (less than 5 x 10^{-4} SI and 2.65 g/cm^3; Fig. 5). Witnesses of these granitic plutons are mapped in the field, bounded and affected by the dextral shearing of the NASZ: the Pertre granite emplaced at 343 ± 3Ma (Verhnet et *al.*, 2009) and the Craon granite (e.g. Le

Gall et *al.*, 2011; Trautmann et *al.*, 2011). The location and the shape of the undercover granites suggest that they probably are affected by the NASZ shearing (Fig. 8c).

Overall, the Central Brittany litho-structural unit, delimited to the south by clear markers of Fe-rich Ordovician sandstones, appears also limited to the east, at the junction between the NASZ and the NBSASZ (Fig. 6b). In the southwestern part of the Paris Basin, these interpretations are consistent with the tectonic sketch of major Armorican shear zones proposed by Martinez Catalàn et *al.*, (2012). The southern part of Central Brittany is structured by patterns of Neoproterozoic and Paleozoic sedimentary rocks. In its northwestern part, the early-Carboniferous Laval basin is developed along the NASZ; it is delimited by low magnetic and gravity signatures (Fig. 6b) related to granitic bodies (Fig. 7a), to the south.

6.2.2 The Lanvaux unit

In agreement with previous works, the eastern extension of the Lanvaux negative gravity anomaly (Fig. 4b) is well documented along more than 200 km (Weber, 1973; Debeglia and Weber, 1980; Autran et *al.*, 1994; Martelet et *al.*, 2013). This anomaly is interpreted as deriving from the low magnetization and low density signatures of the Lanvaux orthogneiss, confirmed by the petrophysical measurements (from 10^{-5} to 0.7×10^{-4} SI and 2.55 g/cm^3; Fig. 5). In the field, the Carboniferous Bécon and the St-Lambert granites display low magnetic susceptibilities and densities comparable to those of the orthogneiss (from 2×10^{-5} to 10^{-4} SI; Fig. 5); it is therefore not possible to discriminate the older Lanvaux orthogneiss (477 ± 18 Ma; Guerrot et al., in Janjou et *al.*, 1998) from the Carboniferous granites. The Carboniferous granites being mainly located along the SBSASZ (Fig. 8c), we consider that the low magnetic and gravity signatures are related to the Lanvaux orthogneiss (Fig. 8c). Eastwards, under cover, the strike of the NW-SE Lanvaux orthogneiss evolves to an E-W and progressively NE-SW direction, parallel to the NBSASZ (Fig. 8c). Lanvaux unit is an antiform (Faure and Cartier, 1998), with Neoproterozoic metasedimentary and Paleozoic sedimentary rocks similar to those of the Central Brittany and with comparable petrophysical characteristics (Fig. 5). The succession of geophysical signatures of metasedimentary and sedimentary rocks as well as the orthogneiss observed in the field extends eastwards under the Paris Basin sedimentary cover. This suggests that the unit has the same antiformal structure, throughout its eastward extension (Fig. 7b). At the southern border of the Lanvaux unit, the magnetic signature of the Paleozoic rocks highlights the tectonic limit with the St-Georges-sur-Loire unit (Fig. 6b).

6.2.3 The St-Georges-sur-Loire unit

Whereas cartographically well marked under cover, the eastern extension of the St-Georges-sur-Loire unit has various geophysical signatures (Fig. 6a), rather magnetic and dense. Cartographically, these signatures cannot be formally related to the northern/southern parts of the unit, as observed in the field (Fig. 2a). The northern part of the unit is marked by low magnetic and gravity signatures (Fig. 6a) related to a granitic pluton (up to 10^{-4} SI and 2.65 g/cm^3; Fig. 5), located at the junction between the Lanvaux and the St-Georges-sur-Loire units, mostly hidden below the Paleozoic series (up to 5×10^{-4} SI and 2.68 g/cm^3). Granites located along the SBSASZ (Fig. 8c) belong to a leucogranite belt displaying dextral shearing, associated with the emplacement of the leucogranite plutons (Berthé et *al*., 1979; Jégouzo, 1980; Vigneresse and Brun, 1983; Gapais et *al*., 1993; Turillot et *al*., 2009). Among them, Questembert and Lizio leucogranites (Fig. 8c) emplaced at 316 ± 3 Ma and 316 ± 6 Ma (Tartèse et *al*., 2011b, 2011a), in agreement with the St-Lambert granite located to the Lanvaux unit, which displays S/C structures suggesting an emplacement during the dextral shearing of the NBSASZ at 312 ± 3 Ma (Faure and Cartier, 1998). Under cover, these low magnetic and gravity signatures are not observed (Fig. 6a), thus these granites cannot be extended eastward, suggesting a limited eastward extension of the leucogranitic belt.

The southern part of the unit, the blocky sub-unit is characterized by scattered high magnetic and various low to high gravity signatures (Fig. 6a). Below the Paris Basin sedimentary cover, the high magnetic and gravity signatures elongated eastwards throughout the map, likely correspond to basic rocks, as interpreted by Martelet et *al.*, (2013). These basic rocks can be variously interpreted in terms of lithology: i) basaltic or gabbroic olistostoliths as described in this unit in the Armorican Massif (Cartier and Faure, 2004), ii) interbedded basalts related to the opening of a back-arc basin (Ducassou et *al.*, 2011) or iii) mafic rocks such as the ophiolites which sporadically crop out along the NSE fault (Marchand, 1981; Faure et *al.*, 2008; Ballèvre et *al.*, 2009). In the eastern part of the St-Georges-sur-Loire unit, the depth of the contact between the substratum and the sedimentary cover is defined at about 500 m, and the bodies responsible for the magnetic signal are located at more than 1500 m depth (Martelet et *al.*, 2013). Consequently the magnetic susceptibility of the magnetic source has to be strong enough to produce such a magnetic signature. According to the magnetic susceptibility measured in the field in St-Georges-sur-Loire unit, we cannot interpret the source as basalts since they do not yield a high magnetic susceptibility (from 6 to 8 x 10^{-4} SI; Fig. 5). The third hypothesis better complies with the petrophysical signatures and with other evidence reported in the literature. Indeed, the interpretation of the Armor2 seismic profile, located in the southern part of the Armorican Massif (Bitri et *al.*, 2003), suggested the presence of the northern part of the Champtoceaux complex beneath St-Georges-sur-Loire unit. The northern part of this complex crops out as ophiolitic series along the NSE fault; it is made of high magnetic susceptibility and high density rocks, such as amphibolite, and micaschists (from 1.1 to 1.5 x 10^{-2} SI, 3.02 g/cm^3 and up to 0.3 SI, 2.79 g/cm^3, respectively; Fig. 5). Therefore, contrary to previous sketch (Weber, 1973; Debeglia and Weber, 1980), our results reveal the eastward extension of ophiolitic series marking the NSE Eo-Variscan suture (Fig. 8d); it is supported by high magnetic and gravity signatures which extend up to the eastern part of the study area limiting St-Georges-sur-Loire unit to the south.

6.2.4 The Mauges nappe and the Champtoceaux Complex

The Mauges nappe, mainly composed of Neoproterozoic micaschists (Fig. 2), exhibits both low magnetic and gravity signatures (Fig. 6a) that may account for hidden granitic plutons. Granitic rocks crop out locally, as for instance the Chemillé pluton intruding the Mauges micaschists, displaying low magnetic susceptibility and density (up to 8 x 10^{-4} SI and 2.55 g/cm^3; Fig. 5). Similar low geophysical signatures depicted in the undercover extension of the Mauges nappes (Fig. 6a) suggest the presence of punctual granitic plutons, probably similar to the Chemillé granite (Fig. 8c). Also, metabasites interbedded in the micaschists yield higher magnetic susceptibility and density ranges (from 5 to 7 x 10^{-4} SI and 2.82 g/cm^3; Fig. 5) than the surrounding micaschists. These signatures trace the eastward extension of the Mauges nappe under the sedimentary cover of the southern part of the Paris Basin (Fig. 7a).

The Choletais area is composed of Cambrian acidic volcanites, intruded by microgranite, granodiorite and gabbro-diorite, unconformably covering the Neoproterozoic rocks (Fig. 2). Among them, the Vézins granodiorite (Fig. 8c) emplaced at 345 ± 5 Ma (Thiéblemont et *al*., 2011) is supposed to be a syn-kinematics intrusion related to the dextral shearing of the

Cholet fault (Rolin et *al.*, 2009). In the Choletais area, the magnetic susceptibilities and density measurements do not discriminate the gabbro-diorite suites from the granodioritic plutons (from 4 to 7 x 10^{-2} SI, 2.83 g/cm^3 and from 2 to 5 x 10^{-2} SI, 2.73 g/cm^3, respectively; Fig. 5). For this reason, these lithologies are grouped together as "basic rocks" in the interpretative geological map (Fig. 7a). The Cambrian volcanics are discrimated by a lower density compared to basic rocks (2.65 g/cm^3 and from 2.73 to 2.83 g/cm^3, respectively; Fig. 5). As previously described (Weber, 1971), in the southern part of the Mauges nappe, the northern branch of the Cholet fault is bounded to the north by an unexpected E-W striking high density elongated anomaly, which extends 200 km eastwards (Fig. 4b). It is superimposed, in the Armorican Massif, to the low magnetization and low density Thouars microgranite (from 1 to 7 x 10^{-4} SI and 2.65 g/cm^3; Fig. 5). The high intensity anomaly can however be explained by the close association of acidic and basic magmatism composing the Thouars massif (Mathieu, 1943, 1958; Weber, 1971) emplaced at 519 ± 10 Ma (Thiéblemont, et *al.*, 2011). The high resolution geophysical data enhance this dual anomaly: it highlights punctual high magnetization signatures associated with high density anomaly (Fig. 6a) related to basics rocks (from 3 to 6 x 10^{-2} SI and up to 2.83 g/cm^3; Fig. 5) and the presence of high density intrusive dolerite (2.97 g/cm^3; Fig. 5) located along the Cholet fault, at the junction between the Mauges nappe and the Haut Bocage unit.

The early Carboniferous Ancenis basin is marked by a low gravity anomaly (Fig. 4b) likely related to a hidden granitic pluton (Fig. 8c) as previously described by Martelet et *al.*, (2013) as well as E-W striking high magnetic trends well defined in the vertical gradient of the magnetic anomaly. This contrast can reasonably be related to the northern extension of the Champtoceaux complex, corresponding to the ophiolitic nappe, buried below the Ancenis basin, along the NSE fault, also interpreted in Armor2 seismic profile (Bitri et *al.*, 2003).

Following the NSE fault to the east, the Permo-Carboniferous Arpheuilles basin, recognized by seismic profiles under cover (Beccaletto et *al.*, 2015) and two boreholes (Fig. 6b), exhibits a peculiar texture in the magnetic first vertical derivative (Fig. 3c) and tilt (Fig. 3d) maps. This texture allows delimiting the extension of the Arpheuilles basin (Fig. 8b). Superimposed on the magnetic texture, high intensity magnetic anomalies are interpreted as the presence of Cambrian volcanic rocks (Fig. 7a) underlying Arpheuilles basin, accompanied by granitic plutons highlighted by their low gravity signatures (Fig. 6a). Our results show that, to the north, Arpheuilles basin is bounded by the NSE fault and controlled by N150E striking faults as well as their N30E-N40E conjugates (Fig. 8b). This suggests that the Arpheuilles basin may be the lateral equivalent of the early Carboniferous Ancenis basin.

6.2.5 The Aigurande Plateau and its connection with the Haut Bocage unit

This area consists in a stack of metamorphic nappes intruded by granitic plutons (Fig. 2). Under cover, the Cholet fault delimits the northern contact of the high grade metamorphic nappes with the Mauges nappe, composed of low grade micaschists (Fig. 8d).

In the northern part of the Aigurande Plateau, the Lower Gneiss Unit (LGU), is mainly composed of low magnetic susceptibility and density micaschists and metagrauwackes (up to 4×10^{-4} SI and 2.8 g/cm^3; Fig. 5), and intermediate magnetic and high density amphibolite (from 5 to 9×10^{-4} SI, 3.01 g/cm^3). The Upper Gneiss Unit (UGU) was discriminated from the LGU by both the high magnetic and density signatures (Fig. 6a) deriving from the amphibolites within the leptynite-amphibolite complex (from 1.5×10^{-2} to 5×10^{-2} SI and 2.98 $g/cm^{3;}$ Fig. 5). Consequently, the LGU/UGU contact can be mapped under the Paris Basin sedimentary cover, bounded to the north by the northern branch of the Cholet fault (Fig. 7a). The LGU micaschists are associated with the Haut Bocage unit described in the field (Fig. 6b; Fig. 7a), which consist of a stack of metamorphic nappes, refolded in an ENE-SSW striking antiform/synform succession, intruded by Carboniferous granites (Fig. 7b).

The micaschists of the Para-autochtonous unit displaying low to intermediate magnetic susceptibility and density (up to 4 x 10^{-4} SI and 2.68 g/cm^3), related to low to intermediate magnetic and gravity signatures (Fig. 6a), has no characteristic signature that can be mapped under the Paris Basin sedimentary cover.

In this area, granitic plutons belong to the Hercynian Mortagne – Marche leucogranites belt (Vigneresse, 1988; Gapais et *al*., 1993; Vigneresse, 1999; Rolin and Colchen, 2001; Rolin et *al.*, 2009; Edel et *al*., 2015; Gapais et *al*., 2015). These granites are largely represented in the Haut Bocage unit and Massif connection (Fig. 7a).

6.2.6 The Poitou High: the Haut Bocage unit and the Confolentais area junction

Largely represented in the field, in the Haut Bocage unit and the Confolentais area (Fig. 6b), the low magnetic and gravity signatures (Fig. 6a) are related to granitic plutons (from 0.8 x 10^{-5} to 10^{-4} SI and 2.65 g/cm^3; Fig. 5). Under cover, equivalent magnetic and gravity signatures related to granitic plutons described in the Poitou High (from 2.5 to 4 x 10^{-5} SI and 2.62 g/cm^3; Fig. 5), mark the connection between the southern part of the Haut Bocage unit and Confolentais area (Fig. 7a). As largely recovered in boreholes (Fig. 6b), granitic plutons represent the main rocks of the substratum in this area (Fig. 7a). These granitic plutons consist in leucomonzogranites, leucogranites, granodiorites and calk-alkaline diorites. They belong to a granitic belt emplaced from late Devonian to early-Carboniferous and are associated with the shearing of the various branches of the SASZ (see Rolin et al., 2009 for more information). Using the geophysical signatures of the substratum (Fig. 6a), it is not possible to discriminate the various leucomonzogranites, leucogranites and granodiorites.

Under the sedimentary cover, the southern part of the Poitou High is marked by punctual high magnetic and gravity signatures (Fig. 6a) related to the calk-alkaline diorite plutons exposed in the field, both in Confolentais area and Haut Bocage unit (Fig. 6b). These diorite plutons emplaced at 373 ± 10 Ma (Cuney et al., 1993) and from 360 ± 3 Ma to 349 ± 5 Ma (Bertrand et al., 2001; Alexandre et al., 2002) for the Montcoutant and various Poitou High diorite plutons, respectively, are associated with the dextral shearing of the SBSASZ (Fig. 8c) (see Rolin et al., 2009 for more information). In the southern Aigurande Plateau, Huriel diorite intrusion (Fig. 8c) emplaced at 361 ± 1 Ma (Pin and Paquette, 2002) and post-date the dextral shearing of the Marche fault (Rolin et al., 2009). Diorite plutons have consistent high magnetic susceptibility and density (up to 1.5 x 10^{-2} SI and 2.80 g/cm^3 and from 3 to 6 x 10^{-3} SI, and 2.80 g/cm^3, respectively; Fig. 5). These basic rocks are discriminated i) from the intermediate magnetic and low density signatures corresponding to the LGU host micaschists, in the Haut Bocage unit, and ii) from the high magnetic and intermediate signatures related to the metavolcanites belonging to the UGU (up to 0.3 SI; Fig. 5), in the Confolentais area (Fig. 7a).

7. Summary and Conclusion

Our paper outlines the benefit of a joint interpretation of potential fields (high-resolution aeromagnetic and gravity data) and petrophysical characterization (magnetic susceptibility and density measurements on rock samples), in order to derive reliable lithological and structural mapping of a buried substratum.

In order to propose a geological map of the hidden substratum of the southwestern part of the Paris Basin, our methodology, is divided into five successive stages: i) the potential field data were processed, with the aim to get specific information (geophysical contrasts, structural features…), ii) magnetic susceptibilities and densities were measured on field rock samples along the eastern border of the Armorican Massif and the northern border of the Massif Central, leading to a petrophysical library of lithologies, iii) using selected magnetic and gravity maps, a map of geophysical signatures was synthetized using an unsupervised classification, featuring 6-levels of magnetic/gravity intensities, iv) the combined analysis and interpretation of magnetic and gravity trends with the synthetized geophysical signatures, allowed extending the Variscan litho-structural units below the Paris Basin sedimentary pile, v) relating the geophysical signatures to the petrophysical characteristics (density and magnetization) within each litho-structural unit, allowed interpreting a geological map of the substratum. This updated study reveals new geological information: i) the limited eastward extension of Central Brittany, bordered to the east by the NE-SW striking NBSASZ; ii) the eastward extension, along ca. 150 km, of the Cholet fault, interpreted as a major fault, delineating the northern limit of the Aigurande Plateau; iii) the emphasis on a series of N150E-N160E and N30E striking normal Variscan fault, reactivated during the tectonic history of the Paris Basin, especially controlling the opening of Permo-Carboniferous basins; iv) the extension of the Nort-sur-Erdre fault considered as an ophiolitic suture, documented by the presence of high magnetic and density rocks along the southern part of the St-Georges-sur-Loire unit.

Overall, our methodology provides keys for extensive mapping of buried basement using magnetic, gravity and petrophysical data. In the near future, this study will be extended to the entire Paris Basin in order to propose a complete geological map of the pre-Mesozoic substratum of the Paris Basin.

Acknowledgments

This work is part of a PhD Thesis co-funded by Région Centre and BRGM. We thank an anonymous reviewer and J.B. Edel for useful and constructive comments, which contributed to improving the manuscript. Geophysical maps were drawn using Geosoft© software.

References

Alexandre, P., Le Carlier de Veslud, C., Cuney, M., Ruffet, G., Virlogeux, D., Cheilletz, A., 2002. Datation 40Ar/39Ar des leucogranites sous couverture du complexe plutonique de Charroux–Civray (Vienne). Comptes Rendus Geoscience 334, 1141–1148. doi:10.1016/S1631-0713(02)01859-X

Autran, A., Lameyre, J., 1980. Conclusions générales. Les granitoïdes de France. Mémoires BRGM 107, 87–99.

Autran, A., Lefort, J.P., Debeglia, N., Edel, J.B., Vigneresse, J.L., 1994. Gravity and Magnetic Expression of Terranes in France and Their Correlation Beneath Overstep Sequences, in: Chantraine, J., Rolet, J., Santallier, D.S., Piqué, A., Keppie, J.D. (Eds.), Pre-Mesozoic Geology in France and Related Areas, IGCP-Project 233. Springer Berlin Heidelberg, pp. 49–72.

Ballèvre, M., Pinardon, J.-L., Kienast, J.-R., Vuichard J.-P., 1989. Reversal of Fe-Mg partitioning between garnet and staurolite in eclogite-facies metapelites from the Champtoceaux nappe (Brittany, France). Journal of Petrology 30, 1321–1349.

Ballèvre, M., Paris, F., Robardet, M., 1992. Corrélations ibéro-armoricaines au Paléozoïque : une confrontation des données paléobiogéographiques et tectonométamorphiques. Comptes Rendus de l'Académie des sciences. Série 2, Mécanique, Physique, Chimie, Sciences de l'univers, Sciences de la Terre 315, 1783–1789.

Ballèvre, M., Marchand, J., Godard, G., Goujou, J.-C., Christian, J., Wyns, R., 1994. Eo-Hercynian Events in the Armorican Massif, in: Chantraine, J., Rolet, J., Santallier, D.S., Piqué, A., Keppie, J.D. (Eds.), Pre-Mesozoic Geology in France and Related Areas, IGCP-Project 233. Springer Berlin Heidelberg, pp. 183–194.

Ballèvre, M., Lardeux, H., 2005. Signification paléoécologique et paléogéographique des bivalves du Carbonifère inférieur du bassin d'Ancenis (Massif armoricain). Comptes Rendus Palevol 4, 109–121. doi:10.1016/j.crpv.2004.11.011.

Ballèvre, M., Bosse, V., Ducassou, C., Pitra, P., 2009. Palaeozoic history of the Armorican Massif: Models for the tectonic evolution of the suture zones. Comptes Rendus Géoscience 341, 174–201. doi:10.1016/j.crte.2008.11.009.

Baptiste, J., Martelet, G., Faure., Beccaletto, L., Perrin, J., 2015. Up-to-date regional gravity and aeromagnetic data to unravel the geological patterns of the pre-Mesozoic substratum of the Paris Basin. Variscan 2015 : The Variscan belt : correlations and plate dynamics, Jun 2015, Rennes, France.

Beccaletto, L., Hanot, F., Serrano, O., Marc, S., 2011. Overview of the subsurface structural pattern of the Paris Basin (France): Insights from the reprocessing and interpretation of regional seismic lines. Marine and Petroleum Geology, Thematic Set on the Implications of basin dynamics on petroleum systems 28, 861–879. doi:10.1016/j.marpetgeo.2010.11.006

Beccaletto, L., Capar, L., Serrano, O., Marc, S., 2015. Structural evolution and sedimentary record of the Stephano-Permian basins occurring beneath the Mesozoic sedimentary cover in the southwestern Paris basin (France). Bulletin de la Société Géologique de France. 6, 429-450.

Bernard-Griffiths, J., Peucat, J.J., Sheppard, S., Vidal, P., 1985. Petrogenesis of Hercynian leucogranites from the southern Armorican Massif: contribution of REE and isotopic (Sr, Nd, Pb and O) geochemical data to the study of source rock characteristics and ages. Earth and Planetary Science Letters 74, 235–250. doi:10.1016/0012-821X(85)90024-X

Berthé, D., Choukroune, P., Jegouzo, P., 1979. Orthogneiss, mylonite and non coaxial deformation of granites: the example of the South Armorican Shear Zone. Journal of Structural Geology 1, 31–42. doi:10.1016/0191-8141(79)90019-1

Bertrand, J.M., Leterrier, J., Cuney, M., Brouand, M., Stussi, J.M., Delaperrière, E., Virlogeux, D., 2001. Géochronologie U-Pb sur zircons de granitoïdes du Confolentais, du massif de Charroux-Civray (seuil du Poitou) et de Vendée. Géologie de la France 1, 167–189.

Bitri, A., Ballèvre, M., Brun, J.-P., Chantraine, J., Gapais, D., Guennoc, P., Gumiaux, C., Truffert, C., 2003. Imagerie sismique de la zone de collision hercynienne dans le Sud-Est du Massif armoricain (projet Armor 2/programme Géofrance 3D). Comptes Rendus Géoscience 335, 969–979. doi:10.1016/j.crte.2003.09.002.

Blakely, R.J. 1996. Potential Theory in Gravity and Magnetic Applications (Cambridge University Press).

Bonijoly, D., Perrin, J., Truffert, C., Asfirane, F., 1999. Couverture géophysique aéroportée du Massif armoricain, magnétisme et radiométrie spectrale. Rapport BRGM R 40471.

Bosse, V., Feraud, G., Ruffet, G., Ballèvre, M., Peucat, J.-J., De Jong, K., 2000. Late Devonian subduction and early-orogenic exhumation of eclogite-facies rocks from the Champtoceaux Complex (Variscan belt, France). Geological Journ*al.* 35, 297–325. doi:10.1002/gj.864.

Burg, J.-P., 1981. "Tectonique tangentielle hercynienne en Vendée littorale : Signification des linéations d'étirement E-W dans les porphyroïdes à foliation horizontale." Comptes Rendus de l'Académie des Sciences de Paris, 293, 849-854.

Cabanis, B., Wyns, R., 1986. Le volcanisme précambrien des Mauges (sud-est du Massif armoricain) et ses caractères géochimiques. Hercynica, Rennes, (II), 1, 71-78.

Cartannaz, C., Rolin, P., Le Métour, J., Fabbri, O., 2006. Fammenian–Tournaisian dextral ductile shear in the French Variscan belt. Comptes Rendus Géoscience 338, 214–221. doi:10.1016/j.crte.2005.12.003

Cartier, C., Faure, M., Lardeux, H., 2001. The Hercynian Orogeny in the South Armorican Massif (Saint-Georges-sur-Loire Unit, Ligerian Domain, France): rifting and welding of continental stripes. Terra Nova. 13, 143–149.

Cartier, C., Faure, M., 2004. The Saint-Georges-sur-Loire olistostrome, a key zone to understand the Gondwana-Armorica boundary in the Variscan belt (Southern Brittany, France). Int. J. Earth Sci. 93, 945–958. doi:10.1007/s00531-004-0398-3.

Cavet, P., Gruet, M., Pillet, J., 1966. Sur la présence du Cambrien à Paroxides à Cléré-sur-Layon (Maine et Loire) dans le Nord-Est du Bocage vendéen (Massif Armoricain). Comptes Rendus Hebdomadaires des séances de l'Académie des Sciences. 263, 1685.

Cavet, P., Arnaud, A., Barbaroux, L., Blaise, J., Brossé, R., Chauris, L., Gruet, M., Lardeux, H., Rivière, J.-M., 1970. Carte géologique de la France (1/50000), *feuille Chalonnes-sur-Loire* (453), BRGM, Orléans.

Cavet, P., Lardeux, H., Philippot, A., 1971. Ordovicien et Silurien aux environs de Montjean et Chalonnes (Maine-et-Loire, Sud-Est du Massif armoricain). Mémoires BRGM 73, 199-212.

Cavet, P., Arnaud, A., Blaise, J., Brossé, R., Chauris, L., Gruet, M., Lardeux, H., 1976. Carte géologique de la France (1/50000), *feuille Angers* (454), BRGM, Orléans.

Chantraine, J., Autran, A., Cavelier, C. and collab., 2003. Carte Géologique de la France au 1/1000000^{e}. BRGM (6$^{\text{ème}}$ édition), Orléans. France.

Chauris, L., and Lucas, G., 1964. Les environs de Bécon-les-Granits (Maine-et-Loire) (Feuille d'Ancenis au 80.000e). Bulletin de la Carte Géologique de France, LX-277 25–33.

Chauris, L., 1969. Sur un important accident structural dans le Nord-Ouest de l'Armorique. Comptes Rendus de l'Académie des Sciences. 268, 2859–2861.

Clark, D., Emerson, D., 1991. Notes on rock magnetization characteristics in applied geophysical studies. Exploration Geophysics 22, 547–555. doi:10.1071/EG991547.

Corpel, J., Weber, C., 1970. Contribution de l'étude de l'aimantation rémanente à la gîtologie du synclinal ferrifère de Segré. Rapport BRGM/70-SGN-029-GPH, 23 pp.

Cuney, M., Stussi, J.-M., Brouand, M., Dautel, D., Michard, A., Gros, Y., Poncet, D., Bouton, P., Colchen, M., Vervialle, J.-P., 1993. Géochimie et géochronologie U/Pb des diorites quartziques du Tallud et de Moncoutant : nouveaux arguments pour une extension de la Ligne Tonalitique Limousine en Vendée. Comptes Rendus de l'Académie des Sciences. Série 2, Mécanique, Physique, Chimie, Sciences de l'univers, Sciences de la Terre 316, 1383–1390.

Dearing, J., 1999. Magnetic susceptibility, in: Environmental Magnetism: A Practical Guide. Quaternary Research Association London, pp. 35–62.

Debeglia, N., Weber, C., 1980. Synthèse géologique du bassin de Paris. Mémoires du BRGM n°102.

Debeglia, N., Weber, C., 1985. Geologic mapping of the basement of the Paris basin (France) by gravity and magnetic data interpretation. In: The Utility of regional gravity and magnetic anomaly maps, (ed. W.J. Hinze). Society of Exploration Geophysicists.

Ducassou, C., Ballèvre, M., Lardeux, H., Robin, C., 2011. Evidence for pre-orogenic, Early Devonian rifting in the Variscan belt: stratigraphy and structure of the Palaeozoic cover of the Mauges Unit (Upper Allochthon, Armorican massif, France). Int. J. Earth Sci. (Geol Rundsch) 100, 1451–1475. doi:10.1007/s00531-010-0605-3.

Edel, J.B., 2008. Structure et nature du socle anté-permien du Bassin de Paris d’après les données gravimétriques et magnétiques – Le problème de l’Anomalie Magnétique du Bassin de Paris (AMBP). Géochronique, 105, pp. 31-37.

Edel, J.-B., Schulmann, K., Lexa, O., Diraison, M., Géraud, Y., 2015. Permian clockwise rotations of the Ebro and Corso-Sardinian blocks during Iberian–Armorican oroclinal bending: Preliminary paleomagnetic data from the Catalan Coastal Range (NE Spain). Tectonophysics 657, 172–186. doi:10.1016/j.tecto.2015.07.002

Elkins, T., 1951. The second derivative method of gravity interpretation. Geophysics. 16, 29–50. doi:10.1190/1.1437648.

Fairhead, J.D., Salem, A., Cascone, L., Hammill, M., Masterton, S., Samson, E., 2011. New developments of the magnetic tilt-depth method to improve structural mapping of sedimentary basins. Geophysical Prospecting 59, 1072–1086. doi:10.1111/j.1365-2478.2011.01001.x.

Faure, M., Prost, A.E., Lasne, E., 1990. Deformation ductile extensive d’age namuro-westphalien dans le plateau d’Aigurande, Massif central francais. Bulletin de la Société Géologique de France VI, 189–197. doi:10.2113/gssgfbull.VI.1.189.

Faure M., Leloix C., Roig J.Y., 1997. L’évolution polycyclique de la chaîne hercynienne. Bulletin de la Société géologique de France 168, 695–705.

Faure, M., and Cartier, C., 1998. Déformations ductiles polyphasées dans l'antiforme orthogneissique de St-Clément-de-la-Place (unité de Lanvaux, Massif armoricain). Comptes Rendus de l'Académie des Sciences - Series IIA - Earth and Planetary Science 326, 795–802. doi:10.1016/S1251-8050(98)80245-0.

Faure, M., Mezeme, E.B., Duguet, M., Cartier, C., Talbot, J.-Y., 2005. Paleozoic tectonic evolution of medio-Europa from the example of the French Massif Central and Massif Armoricain. Journal of the virtual Explorer 19, 1–25.

Faure, M., Bé Mézème, E., Cocherie, A., Rossi, P., Chemenda, A., Boutelier, D., 2008. Devonian geodynamic evolution of the Variscan Belt, insights from the French Massif Central and Massif Armoricain. Tectonics 27, TC2005. doi:10.1029/2007TC002115.

Faure M., 2014. Le substratum de la France métropolitaine : de la formation du Gondwana à la constitution de la Pangée, une histoire de 600 Ma. Géologues, 180, pp. 13-21.

Gapais, D., Lagarde, J.L., Le Corre, C., Audren, C., Jegouzo, P., Casas Sainz, A., Van Den Driessche, J., 1993. La zone de cisaillement de Quiberon: témoin d'extension de la chaine varisque en Bretagne méridionale au Carbonifère. Comptes Rendus de l'Académie des Sciences, Paris, série II 316, 1123–1129.

Gapais, D., Brun, J.-P., Gumiaux, C., Cagnard, F., Ruffet, G., Veslud, C.L.C.D., 2015. Extensional tectonics in the Hercynian Armorican belt (France). An overview. Bulletin de la Société Géologique de France 186, 117–129. doi:10.2113/gssgfbull.186.2-3.117

Gébelin, A., Brunel, M., Monié, P., Faure, M., Arnaud, N., 2007. Transpressional tectonics and Carboniferous magmatism in the Limousin, Massif Central, France: Structural and 40Ar/39Ar investigations. Tectonics 26.

Gérard, A., and Griveau, P., 1972. Interpretation quantitative en gravimétrie ou magnétisme à partir de cartes transformées en gradient vertic*al.* Geophysical Prospecting 20, 459–481. doi:10.1111/j.1365-2478.1972.tb00648.x.

Goguel, J., and Francia, 1954. Levé gravimétrique détaillé du Bassin parisien. Ministère de l'Industrie et de l'Energie. Direction des Mines. Imprimerie Nationale.

Goguel, J., 1972. Tendances modernes dans l'interprétation géologique des données gravimétriques. Bull. BRGM 43–50.

Guillocheau, F., Robin, C., Allemand, P., Bourquin, S., Brault, N., Dromart, G., Friedenberg, R., Garcia, J.-P., Gaulier, J.-M., Gaumet, F., others, 2000. Meso-Cenozoic geodynamic evolution of the Paris Basin: 3D stratigraphic constraints. Geodinamica Acta 13, 189–245.

Houlgatte, E., Le Hérissé, A., Pelhate, A., Rolet, J., 1988. Evolution géodynamique du Bassin carbonifère de Lav*al.* Géologie de la France 1, 27–46.

Jégouzo, P., 1980. The South Armorican Shear Zone. Journal of Structural Geology, Shear zones in rocks 2, 39–47. doi:10.1016/0191-8141(80)90032-2.

Lardeux, H., Cavet, P., 1994. Paleozoic of the Ligerian Domain, in: Chantraine, J., Rolet, J., Santallier, D.S., Piqué, A., Keppie, J.D. (Eds.), Pre-Mesozoic Geology in France and Related Areas, IGCP-Project 233. Springer Berlin Heidelberg, pp. 152–156.

Lecoanet, H., Lévêque, F., Segura, S., 1999. Magnetic susceptibility in environmental applications: comparison of field probes. Physics of the Earth and Planetary Interiors 115, 191–204. doi:10.1016/S0031-9201(99)00066-7.

Le Corre, C., Auvray, B., Ballèvre, M., & Robardet, M., 1991. Le massif armoricain. Scientifical Geological Bulletin. 44, 31-103.

Le Gall, J., Vernhet, Y., Lacquement, F., Gauquelin, J.-L., Robert, A., Cocherie, A., Naveau, J, 2011 – Notice explicative, Carte géologique de France (1/50 000), feuille Laval (319). Orléans : BRGM, 261 p. Carte géologique par Le Gall J., Gigot P., Savaton P., Lacquement F., Poprawsky Y., Vernhet Y. (2011).

Le Hébel, F., Vidal, O., Kienast, J.-R., Gapais, D., 2002. Les « Porphyroïdes » de Bretagne méridionale : une unité de HP–BT dans la chaîne hercynienne. Comptes Rendus Geoscience 334, 205–211. doi:10.1016/S1631-0713(02)01746-7.

Le Hérissé, A., and Plaine, J., 1982. Volcanisme basique dans le Carbonifère inférieur du Synclinorium de Laval (Massif armoricain, France). Comptes Rendus de l'Académie des Scences de Paris, 294, 1199-1202.

Lienhardt, M.J., 1961. Étude stratigraphique, pétrographique et structurale du socle anté permien du bassin de Paris. Annales de la Société Géologique du Nord 81, 233-241.

Marchand, J., 1981. Ecaillage d'un "mélange tectonique" profond: le complexe cristallophyllien de Champtoceaux (Bretagne méridionale). Comptes Rendus de l'Académie des Sciences de Paris 293, 223–228.

Martelet, G., Debeglia, N., Truffert, C., 2002. Updating and validating the French gravity terrain corrections out to a distance of 167 km. Comptes Rendus Géoscience. 334, 449–454.

Martelet, G., Calcagno, P., Gumiaux, C., Truffert, C., Bitri, A., Gapais, D., Brun, J.P., 2004. Integrated 3D geophysical and geological modelling of the Hercynian Suture Zone in the Champtoceaux area (south Brittany, France). Tectonophysics 382, 117–128. doi:10.1016/j.tecto.2003.12.009.

Martelet, G., Pajot, G., Debeglia, N., 2009. Nouvelle carte gravimétrique de la France; RCGF09 – Réseau et Carte Gravimétrique de la France, 2009. Rapport BRGM/RP-57908-FR, 77 p.

Martelet, G., Perrin, J., Truffert, C., Deparis, J., 2013. Fast mapping of magnetic basement depth, structure and nature using aeromagnetic and gravity data: combined methods and their application in the Paris Basin: Fast mapping of a buried basement using magnetic and gravity data. Geophysical Prospecting 61, 857–873. doi:10.1111/1365-2478.12024.

Martínez Catalán J.R., 2012. The Central Iberian arc, an orocline centered in the Iberian Massif and some implications for the Variscan belt. Int. J. Earth Sci. 101, 1299-1314. doi:10.1007/s00531-011-0715-6.

Mathieu, G., 1943. Révision de la feuille de Saumur au 1/80000ème. Bulletin du Service de la Carte géologique de France, 212, p119-129.

Mathieu, G., 1958. Les grandes lignes de la Vendée. Ibid., 253, 46p.

Matte, P., 1986. Tectonics and plate tectonics model for the Variscan belt of Europe. Tectonophysics 126, 329–374. doi:10.1016/0040-1951(86)90237-4.

Matte, P., Hirn, A., 1988. Seismic signature and tectonic cross section of the Variscan crust in western France. Tectonics 7, 141–155.

Matte, P., 1991. Accretionary history and crustal evolution of the Variscan belt in Western Europe. Tectonophysics 196, 309–337. doi:10.1016/0040-1951(91)90328-P.

Mégnien, C., 1980. Synthèse géologique du Bassin de Paris, I, Stratigraphie et paléogéographie, Mémoires du BRGM, 101, 466pp.

Miller, H. G. and Singh, V., 1994. Potential field tilt; a new concept for location of potential field sources. Journal of Applied Geophysics. 32, 213–217.

Peiffer, M.-T., 1986. La signification de la ligne tonalitique du Limousin. Son implication dans la structuration varisque du Massif Central français. Comptes Rendus de l'Académie des Sciences. Série 2, Mécanique, Physique, Chimie, Sciences de l'univers, Sciences de la Terre 303, 305–310.

Perrodon, A. and Zabek, J., 1990. Paris Basin; Interior cratonic basins. AAPG Memoir, 51, 633-679.

Pin, C., and Paquette, J.-L., 2002. Le magmatisme basique calcoalcalin d'âge dévono-dinantien du nord du Massif Central, témoin d'une marge active hercynienne : arguments géochimiques et isotopiques Sr/Nd. Geodinamica Acta 15, 63–77. doi:10.1016/S0985-3111(01)01079-8.

Pomerol, C., 1978. Paleogeographic and structural evolution of the Paris Basin, from the Precambrian to the present day, in relation to neighboring regions. Geologie En Mijnbouw Journal of Geosciences, 57, 533-543.

Quenardel, J.-M., Rolin, P., 1984. Palaeozoic evolution of the Plateau d'Aigurande (NW Massif Central, France). Geological Society, London, Special Publications 14, 63–70. doi:10.1144/GSL.SP.1984.014.01.06.

Rolin, P., Colchen, M., 2001. Les cisaillements hercyniens de la Vendée au Limousin. Géologie de la France, n° 1-2. 87-116.

Rolin, P., Marquer, D., Colchen, M., Cartannaz, C., Cocherie, A., Thiery, V., Quenardel, J.-M., Rossi, P., 2009. Famenno-Carboniferous (370-320 Ma) strike slip tectonics monitored by syn-kinematic plutons in the French Variscan belt (Massif Armoricain and French Massif Central). Bulletin de la Société Géologique de France 180, 231–246. doi:10.2113/gssgfbull.180.3.231.

Tartèse, R., Boulvais, P., Poujol, M., Vigneresse, J.-L., 2011a. Granite petrogenesis revealed by combined gravimetric and radiometric imaging. Tectonophysics 501, 98–103. doi:10.1016/j.tecto.2011.02.003

Tartèse, R., Poujol, M., Ruffet, G., Boulvais, P., Yamato, P., Košler, J., 2011b. New U-Pb zircon and 40Ar/39Ar muscovite age constraints on the emplacement of the Lizio syn-tectonic granite (Armorican Massif, France). Comptes Rendus Geoscience 343, 443–453. doi:10.1016/j.crte.2011.07.005

Taylor, H.L., Mason, M.C., 1972. A Systematic Approach to Well Surveying Calculations. Society of Petroleum Engineers Journal 12, 474–488. doi:10.2118/3362-PA.

Théveniaut, H., Clarke, B., 2013. Large scale magnetic susceptibility soil mapping: a proxy for geological mapping and exploration from Bogoso (Ghana). Exploration Geophysics 44, 48. doi:10.1071/EG12019.

Thiéblemont, D., Cabanis, B., Le Métour, J., 1987. Étude géochimique d'un magmatisme de distension intracontinentale: la série bimodale ordovico-silurienne du Choletais (Massif vendéen), Géologie de la France 1, 65–76.

Thiéblemont, D., Guerrot, C., Le Métour, J., Jézéquel, P., 2001. Le complexe de Cholet-Thouars: un ensemble volcano-plutonique cambrien moyen au sein du bloc précambrien des Mauges. Géologie de la France, n°1-2. 7-17.

Thiéblemont, D., Augier, R., Ferry, J.-N., Laurent-Charvet, S., Maleyx, C., Ravoux, A., Lebret, P., Guerrot, C., Chretien, P., 2011 – Notice explicative, Carte géologique de. France (1/50 000), feuille Vihiers (511). Orléans : BRGM, 122 p.

Trautmann, F., Lacquement, F., Vernhet, Y., Pivette, B., avec la collaboration de Cocherie A., Guerrot C., Thiéblemont D., Tegyey M., Denis E., 2011. – Notice explicative, Carte géologique de France (1/50 000), feuille Vitré (318). Orléans : BRGM, 131 p. Carte géologique par Lacquement F., Trautmann F., Vernhet Y. (2011).

Truffert, C., Gumiaux, C., Chantraine, J., Perrin, J., Galdeano, A., Gapais, D., Ballèvre, M., Asfirane, F., Guennoc, P., Brun, J.-P., 2001. Levé géophysique aéroporté dans le Sud-Est du Massif armoricain (programme GéoFrance3D Armor2). Magnétisme et radiométrie spectrale. Comptes Rendus de l'Académie des Sciences-Series IIA-Earth and Planetary Science 333, 263–270.

Turrillot, P., Augier, R., Faure, M., 2009. The top-to-the-southeast Sarzeau shear zone and its place in the late-orogenic extensional tectonics of southern Armorica. Bulletin de la Société Géologique de France 180, 247–261. doi:10.2113/gssgfbull.180.3.247

Venkateswarlu, N.B., Raju, P.S.V.S.K., 1992. Fast isodata clustering algorithms. Pattern Recognition 25, 335–342. doi:10.1016/0031-3203(92)90114-X

Verduzco, B., Fairhead, J.D., Green, C.M., MacKenzie, C., 2004. New insights into magnetic derivatives for structural mapping. The Leading Edge 23, 116–119.

Vernhet, Y., Plaine, J., Trautmann, F., Pivette, B., avec la collaboration de Chevremont, P., Bourdillon, C., Cocherie, A., 2009 – Notice explicative, Carte géologique de France (1/50 000), feuille Cossé-le-Vivien (355). Orléans : BRGM, 222 p. Carte géologique par Vernhet, Y., Plaine, J., Trautmann, F., Clément J.P., 2009.

Vidal, P., 1980. L'évolution polyorogénique du Massif Armoricain : apport de la géochronologie et de la géochimie isotopique du strontium. Mémoire de la Société géologique Minérale de Bretagne, Rennes, 21,162-958

Vigneresse, J.-L., Brun, J.-P., 1983. Les leucogranites armoricains marqueurs de la deformation regionale; apport de la gravimetrie. Bulletin de la Société Géologique de France S7–XXV, 357–366. doi:10.2113/gssgfbull.S7-XXV.3.357

Vigneresse, J.-L., 1988. La fracturation post-hercynienne du Massif armoricain d'après les données géophysiques. Géologie de la France 4, 3–10.

Vigneresse, J.L., 1999. Intrusion level of granitic massifs along the Hercynian belt: balancing the eroded crust. Tectonophysics 307, 277–295. doi:10.1016/S0040-1951(99)00104-3

Virlogeux, D., Roux, J. ets Guillemot, D., 1999. Apport de la géophysique à la connaissance géologique du Massif de Charroux-Civray et du socle Poitevin. Dans « Etude du Massif de Charroux-Civray ». Actes Journées Sciences CNRS-ANDRA, Poitiers, 13-14. 10,33-61.

Watts, M.S., and Williams, G.D., 1979. Faults rocks as indicators of progressive shear deformation in the Guingamp region, Brittany. Journal of Structural Geology, 1, 323-332.

Weber, C., 1971. Le socle antépermien sous la bordure sud du bassin de Paris d'après les données géophysiques. Bulletin BRGM, section I n°3, 177–189.

Weber, C., 1973. Le socle antétriasique sous la partie sud du Bassin de Paris d'après les données géophysiques. Bulletin BRGM, sect. II, n°3 et 4, 219-343.

Wyns, R., Le Métour, J., 1983. Le Précambrien du massif vendéen. Etude détaillée de deux coupes de référence (coupes de l'Evre et de la Divatte) et synthèse des données récentes. Document BRGM, 68.

Wyns, R., Lardeux, H., Moguedet, G., Duermael, G., Gruet, M., Biagi, R. avec la collaboration de Ballèvre, M., Chevremont, P., 1998. Notice explicative, carte géologique de la France (1/50 000), feuille Chemillé (483). BRGM, Orléans, 72 p.

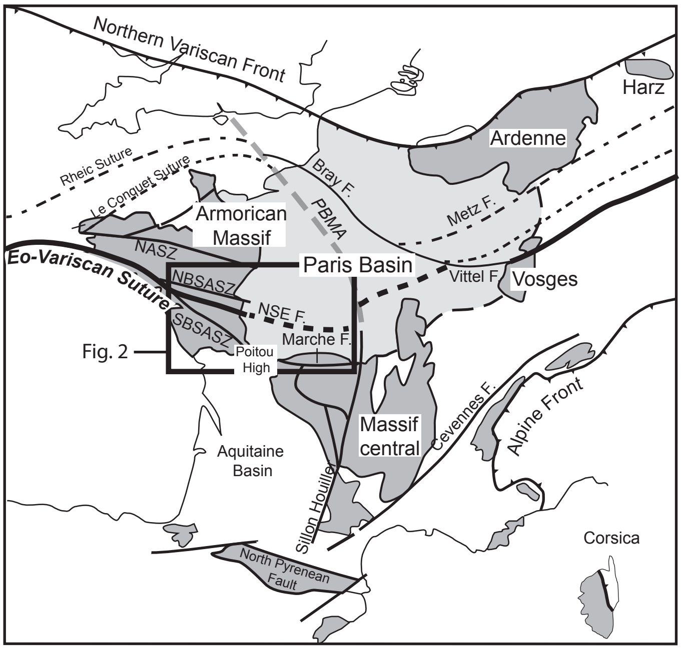

Fig. 1: Map of the Pre-Permian basement in France with Variscan sutures (modified from Faure, 2014). In dark grey: outcrops of the Variscan basement. NASZ: North Armorican Shear Zone, NBSASZ: Northern Branch of the South Armorican Shear Zone, SBSASZ: Southern Branch of the South Armorican Shear Zone, NSE F: Nort sur-Erdre Fault corresponding to the Eo-Variscan suture, PBMA: Paris Basin Magnetic Anomaly. In light grey: outcrop of the Meso-Cenozoic Paris Basin.

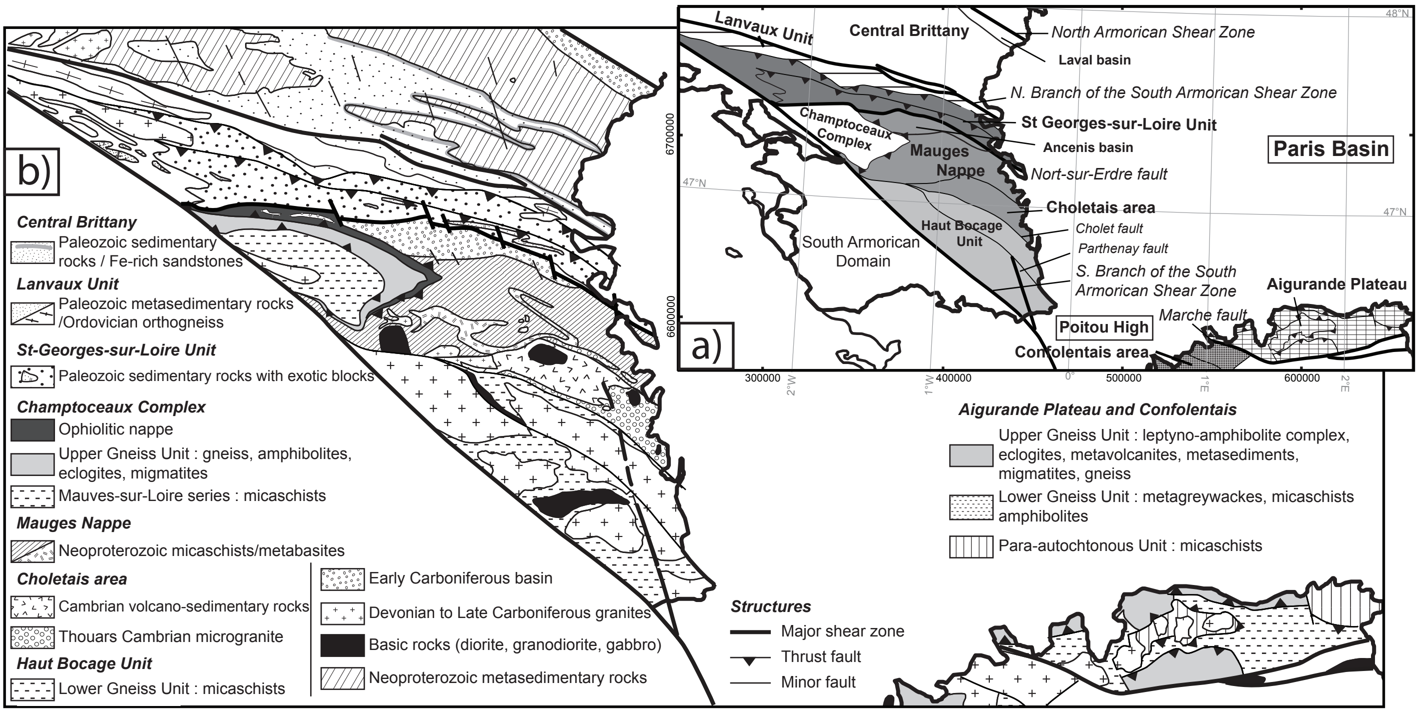

Fig. 2: Geological map of the southeastern part of the Armorican Massif and the northwestern part of the Massif Central: a) Major structures and litho-structural unit delimitations, b) Main lithologies within the litho-structural units (modified from Chantraine et al., 2003).

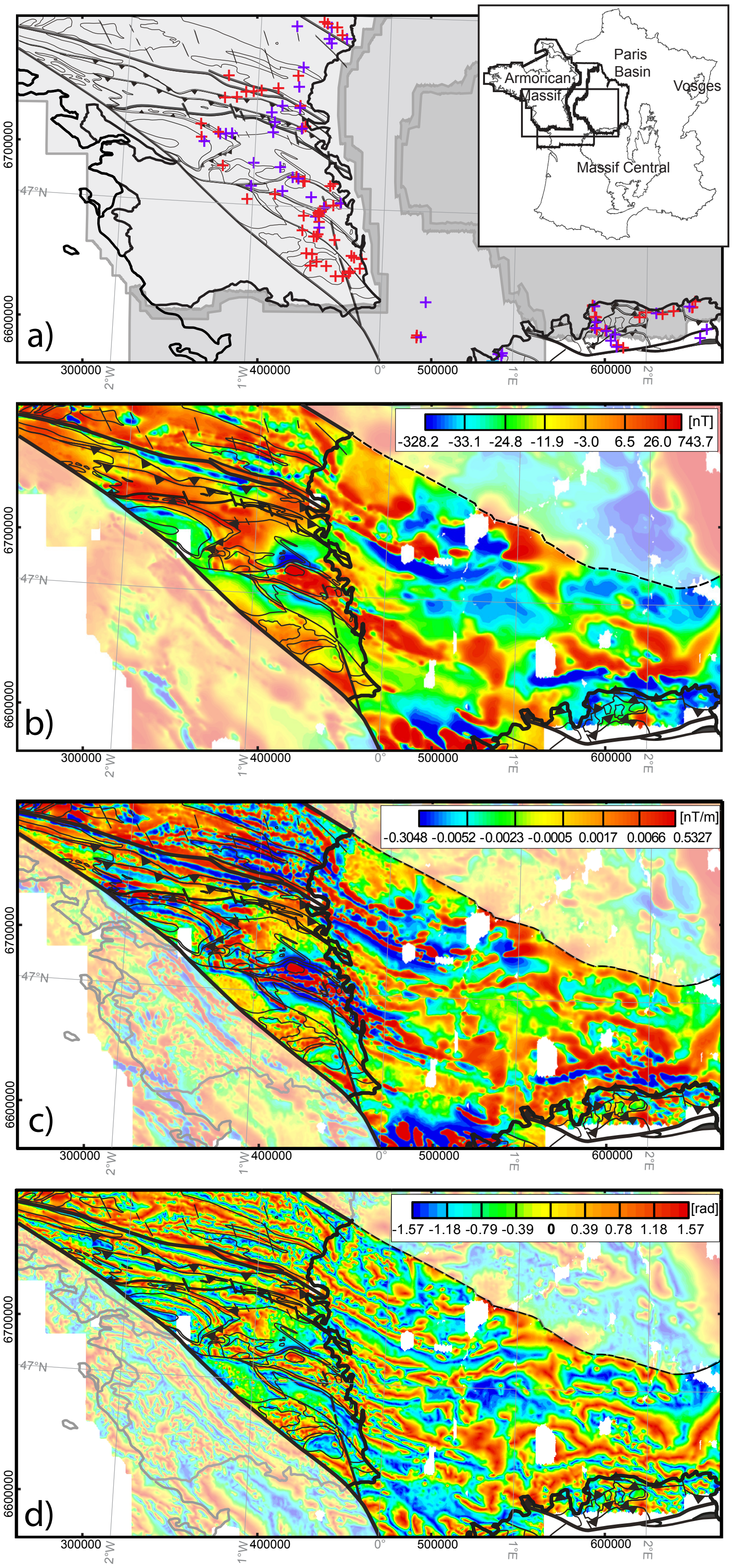

Fig. 3: **a)** Location map of the three aeromagnetic surveys used in this study. From west to east: Brittany, Pays de Loire (PaL), Région Centre. Crosses: location of the petrophysical field samples: in red: magnetic susceptibility only, in purple: magnetic susceptibility and density. **b)** Map of the magnetic anomaly reduced to the pole. **c)** Map of the magnetic vertical gradient. **d)** Map of the magnetic tilt derivative. Structural and lithological contours (thin black lines) and massif boundaries (thick black lines) are superimposed (modified from Chantraine et al., 2003).

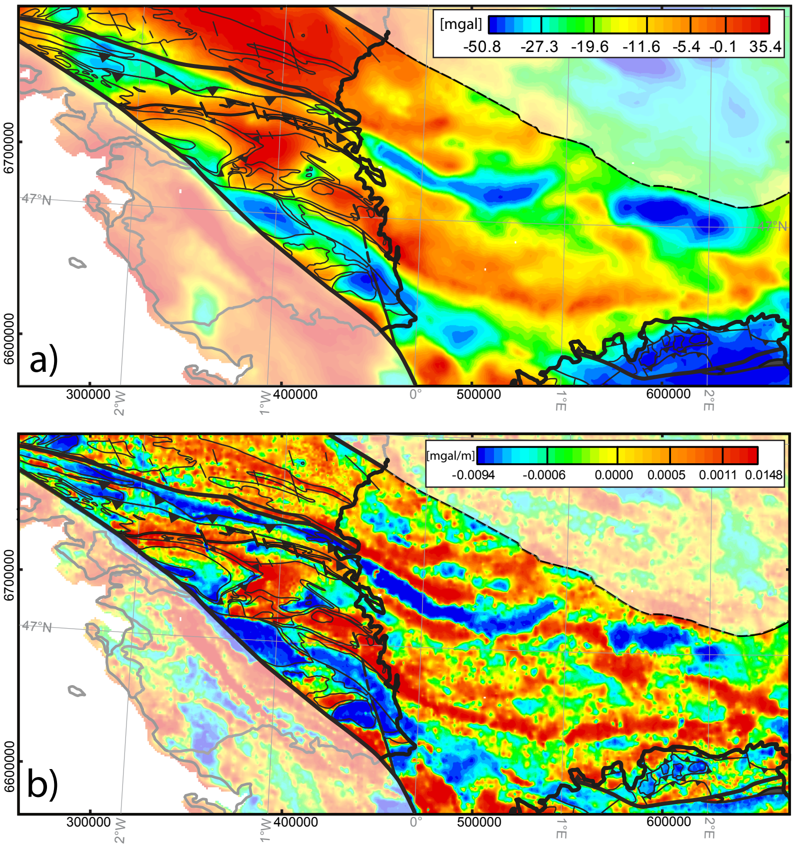

Fig. 4: **a)** Map of the Bouguer anomaly. **b)** Map of the vertical gradient of the Bouguer anomaly. Structural and lithological contours (thin black lines) and massif boundaries (thick black lines) are superimposed (modified from Chantraine et al., 2003).

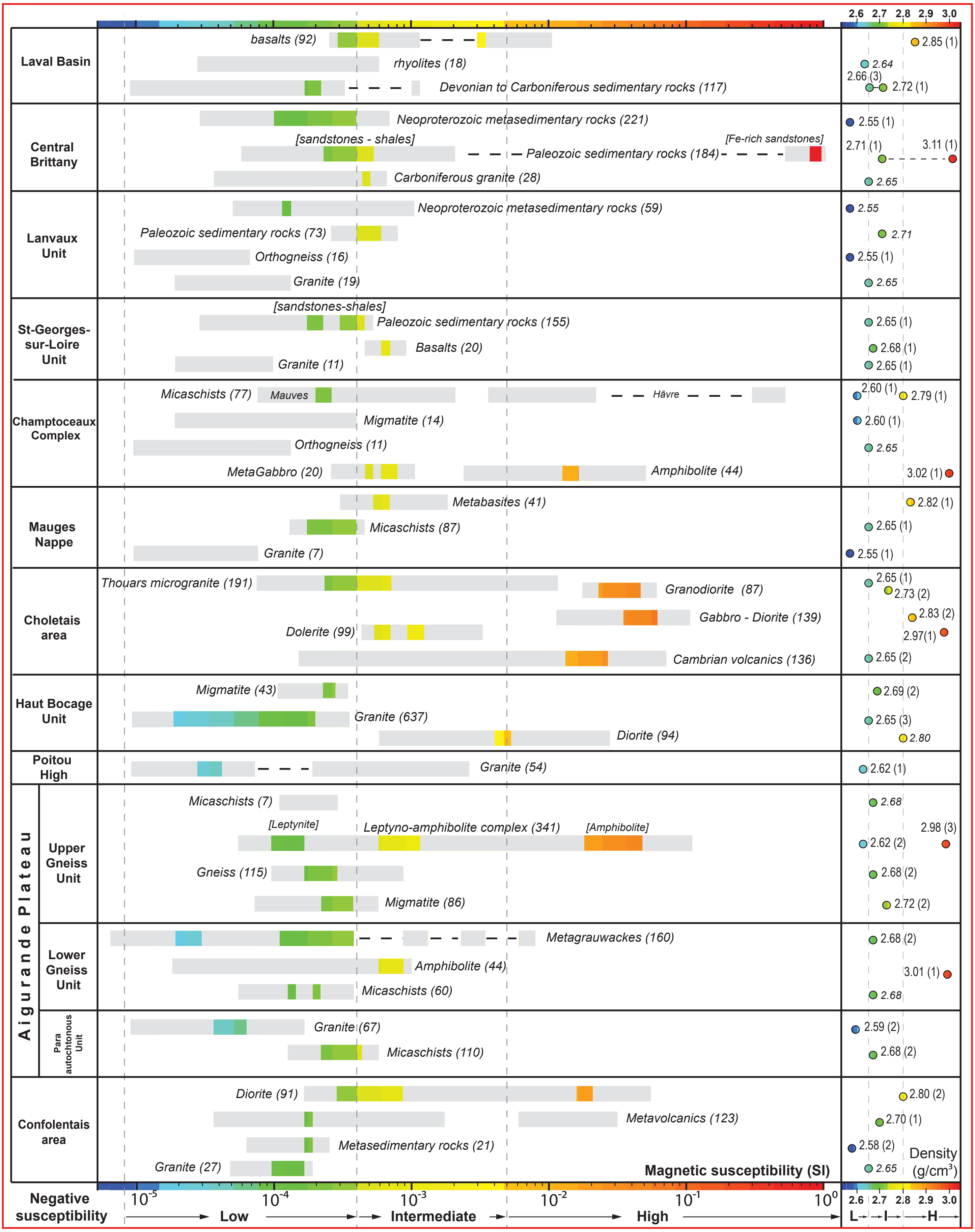

Fig. 5: Magnetic susceptibilities and average density values of the main lithologies sampled in the field, within each litho-structural unit. L: Low, I: Intermediate; H: High densities: refer to the text for explanations. In brackets: number of magnetic susceptibility measurements and number of density samples. Location of the sampling sites is documented in Fig. 3a.

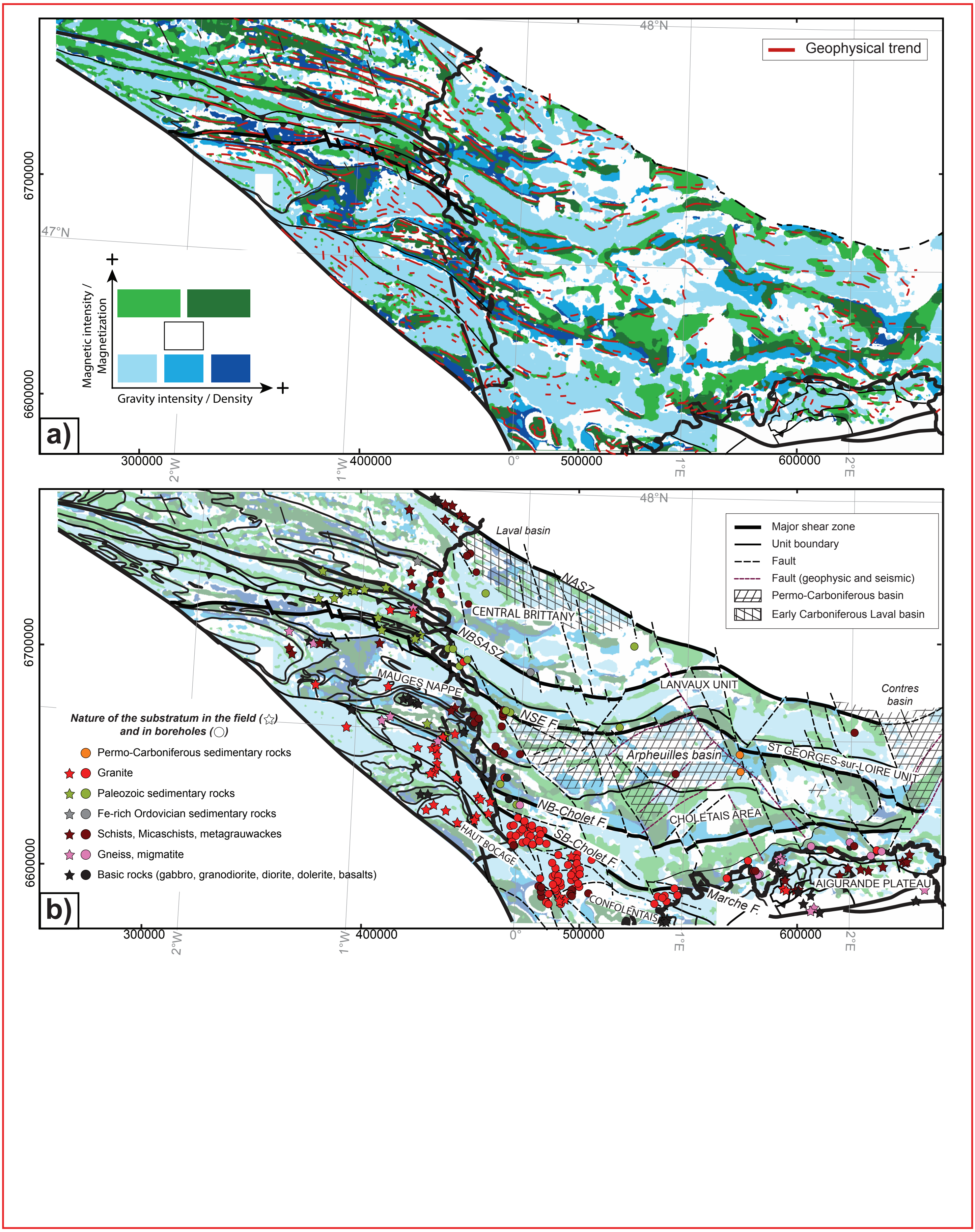

Fig. 6: a) Map of synthetized geophysical signatures resulting from the classification of the magnetic (magnetic anomaly reduced to the pole and magnetic tilt derivative) and gravity (vertical gradient of the Bouguer anomaly) signatures. Magnetic and gravity trends are superimposed (red lines).
b) Interpretative structural sketch map of the Pre-Mesozoic substratum, of the southwestern part of the Paris Basin, with the location of the Permo-Carboniferous basins, the lithology of the studied outcrops (colored stars) and the lithology of the substratum in boreholes (colored circles).

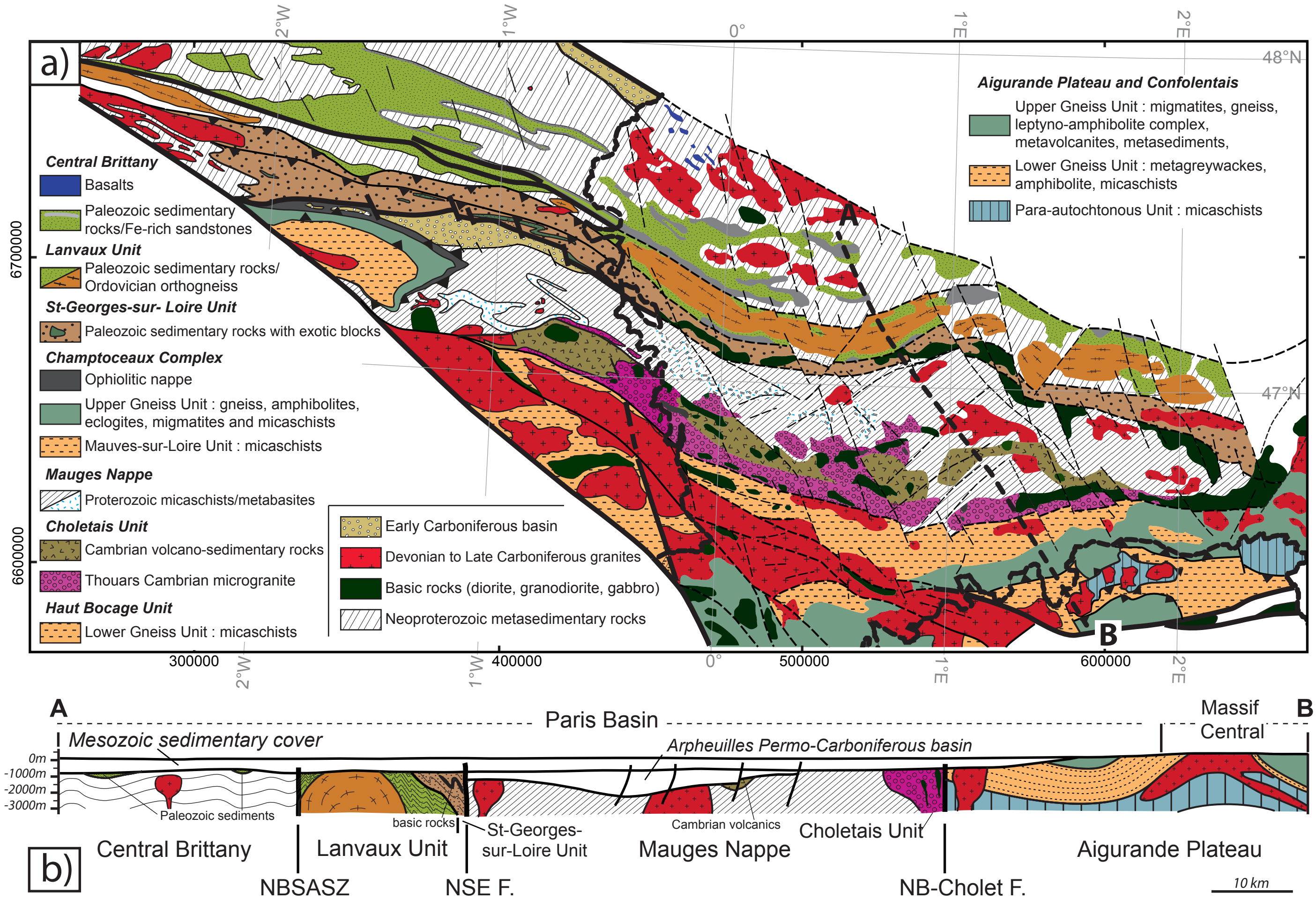

Fig. 7: **a)** Interpretative geological map of the Pre-Mesozoic substratum of the southwestern part of the Paris Basin. This map synthesizes the information coming from the potential field data (aeromagnetic and gravity enhanced maps), the classified geophysical signatures, the structural sketch map and the petrophysical characteristics of rock samples. For clarity reasons, Permo-Carboniferous basins are not represented in this map. The thick black dotted line locates the cross section presented in Fig.7b.
b) Interpretative geological cross-section of the Pre-Mesozoic substratum of the southwestern part of the Paris Basin inferred from the geophysical information processed in this study, and the extension of the structures known in the field.

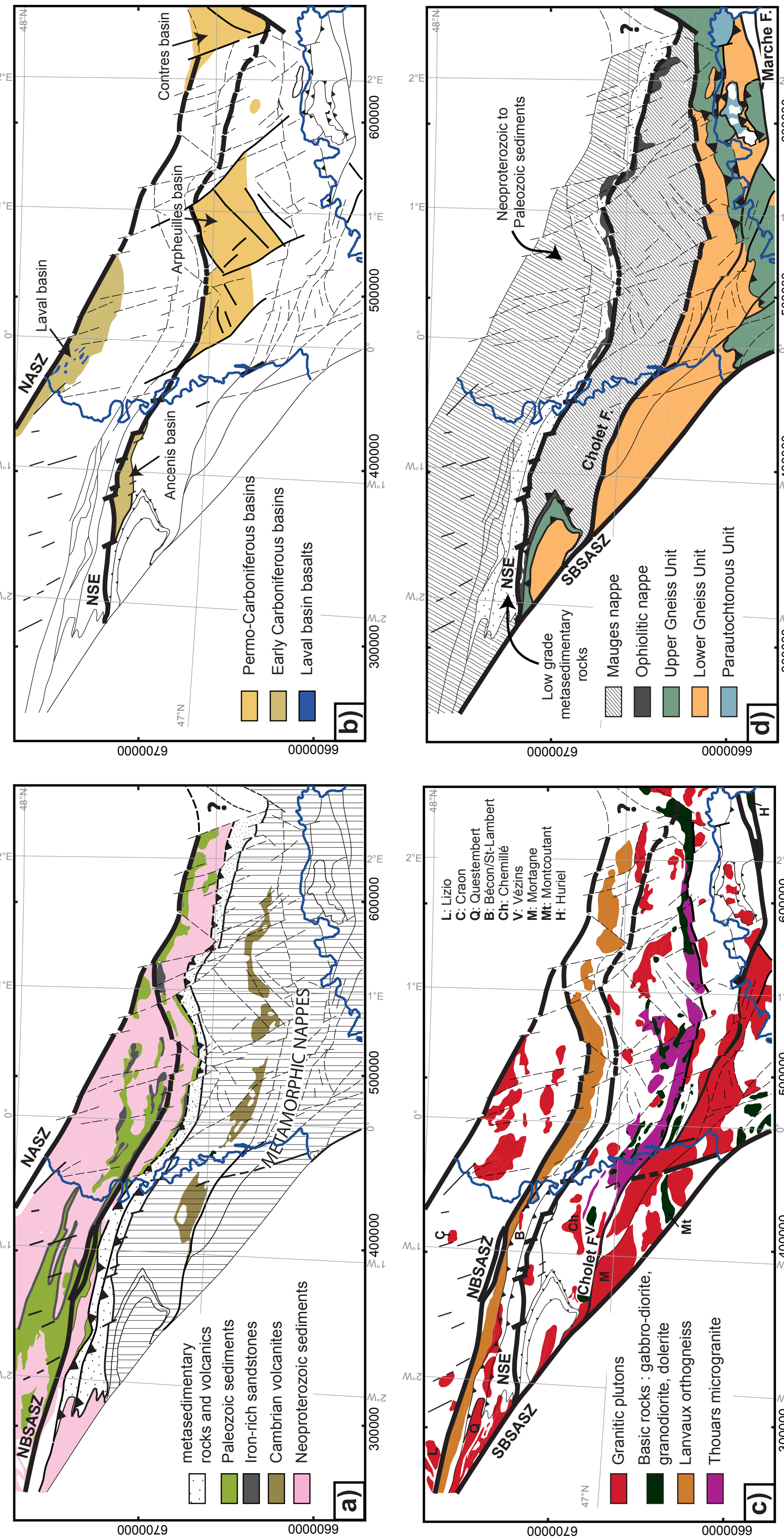

Fig. 8: Decomposition of the geological map into its main lithological ensemble: **a)** Sedimentary rocks and volcanites; **b)** Permo-Carboniferous basins, using geophysical and seismic data (modified from Beccaletto et al., 2015); **c)** magmatic intrusions; **d)** metamorphic nappes. Blue lines : massif boundaries (modified from Chantraine et *al*., 2003)